In presenting this dissertation in partial fulfillment of the requirements for an advanced degree at Idaho State University, I agree that the Library shall make it freely available for inspection. I further state that permission for extensive copying of my dissertation for scholarly purposes may be granted by the Dean of Graduate Studies, Dean of my academic division, or by the University Librarian. It is understood that any copying or publication of this dissertation for financial gain shall not be allowed without my written permission.

Signature_____

Date 6/15/2017

A SINGLE CHAMBER MICROBIAL FUEL CELL USING MULTIPLE ANODE PLATES MADE OF CONDUCTIVE BAMBOO CHARCOAL

by

Rishika Haynes

A dissertation

submitted in partial fulfillment

of the requirements for the degree of

Doctor of Philosophy in the Department of Civil and Environmental Engineering

Idaho State University

Summer 2017

To the Graduate Faculty:

The members of the committee appointed to examine the dissertation of Rishika Haynes find it satisfactory and recommend that it be accepted.

Chikashi Sato, Ph.D.
Major Advisor

Marco Schoen, Ph.D.
Committee Member

Jeffrey Rosentreter, Ph.D.
Committee Member

James Lai, Ph.D.
Committee Member

Martine Beachboard, Ph.D.
Graduate Faculty Representative

Acknowledgements

A continuous journey towards fulfilling my academic goal would not have been possible without the help and support of these very best people in my life. This journey has been remarkable, and today, to be able to write these thank you notes, is very fulfilling.

My utmost respect and gratitude go towards my advisor, Dr. Chikashi Sato, who provided me with guidance and support throughout this course. The support, constructive comments and encouragement from all of the committee members are greatly appreciated.

I want to thank my husband, Christopher Haynes, for his unwavering support. My two children who provided me with unspoken motivation, a tremendous amount of zeal and zest for somebody so little, is simply unexplainable. With these people in my life, tough hasn't become so tough.

Dedication

To my children Swav and Ru

Table of Contents

List of Figures

List of Tables

List of Abbreviations

EAB..... Electrochemically Active Bacteria
DAS..... Data Acquisition System
BOD_5.....5-day Biochemical Oxygen Demand
PMS.....Power Management System
CP.....Carbon Paper
BC ..... Bamboo Charcoal
MAP ..... Multiple Anode Plates
MFC .....Microbial Fuel Cell
DCMFC.....Dual Chamber MFC
SCMFC ..... Single Chamber MFC
MAP-SCMFC ..... SCMFC with MAP
MAP-SCMFC-A .....MAP-SCMFC with designation A
MAP-SCMFC-B .....MAP-SCMFC with designation B
SMFC-A..... MAP-SCMFC-A with one BC anode utilized
SMFC-B ..... MAP-SCMFC-B with one BC anode utilized
SMFC-AB .....SMFC-A and SMFC-B connected in series
EH/SMFC-AB..... SMFC-AB connected in series with an Energy Harvester
MMFC-A .....MAP-SCMFC-A with all anodes utilized
MMFC-B.....MAP-SCMFC-B with all anodes utilized
MMFC-AB.....MMFC-A and MMFC-B connected in series
EH/MMFC-AB ..... MMFC-AB connected in series with an Energy Harvester

Dissertation Abstract

Two single-chamber microbial fuel cells (MFCs) with multiple-anode plates (MAP-SCMFC) were constructed. Each MFC consisted of an anode chamber, a carbon cloth (Pt-coated) cathode, a carbon paper (CP) anode, and four bamboo-charcoal (BC) anode plates. The circuit configurations allowed continuous and simultaneous voltage measurements with five anodes individually or grouped together and with the capability to connect both MFCs in series. The SCMFCs were operated in a draw-and-feed mode using acclimated anaerobic sludge as inoculum and potato-processing wastewater as substrate. The overall research comprised of two parts. The first part of the study evaluated MFC performance with respect to the electrode spacing in an MAP- SCMFC. The largest maximum power density and smallest internal resistance were produced with the anode closest to the cathode, and the smallest maximum power density and largest internal resistance with the anode farthest from the cathode. When all the anodes (CP and BCs) were connected together, the power output increased more than an order of magnitude, from 45 mW/cm^2 with the CP anode to 504 mW/cm^2 with all anodes together, and the internal resistance decreased from 372 to 118 Ω. In the second part of the study, an energy harvester was placed in the circuit configuration to harvest and store power in a capacitor and battery. The highest power produced by the MFCs, when they were placed in series with all the anodes connected together in each of the MFCs (MMFC-AB), was 1328 mW/m^2 with respect to cathode area. The power density with respect to anode area (13 mW/m^2) produced by MMFC-AB configuration was similar to that produced by the MFCs with one BC anode.

CHAPTER 1

Introduction

A microbial fuel cell (MFC) is a device that produces electricity via direct conversion of reduced chemical compounds with the help of microorganisms. Electrochemically active bacteria (EAB) are used as biocatalyst to convert chemical energy of biodegradable compounds into electrical energy. MFCs are innovative devices that possess great potential in treating wastewater and generating electricity simultaneously (Corbella *et al*., 2015). The two-chambered or dual-chamber MFCs (DCMFC) and the single-chamber MFCs (SCMFC) are the fundamental types. A DCMFC consists of an anode chamber (with an anode terminal), a cathode chamber (with a cathode terminal), a proton exchange (or a cation specific) membrane, an external circuit (conductive wire), microorganisms (biocatalysts), substrate (anolyte), and catholyte. The SCMFC eliminates the cathode chamber and catholyte from the MFC design by directly exposing one side of the cathode to the atmosphere and the other side to the anolyte and EAB. An air-cathode allows oxygen (O_2) in air to contact with protons (H^+) in the anode chamber to form water (H_2O) at the cathode surface.

MFC Applications

Microbial fuel cells can treat wastewater while recovering energy from the wastewater (Logan and Rabaey, 2012). While fundamental applications of MFCs are treatment of wastewater and production of electricity, many other applications have emerged over the years. The electrical energy harvested from an MFC can be stored in rechargeable devices such as capacitors and batteries, which are then used for various electrical devices (Dewan *et al.*, 2010; Shantaram *et al.*, 2005). MFCs have been used as biosensors

to monitor pollutants present in wastewater (Chang *et al.*, 2004) and to power wireless sensors (Donovan *et al.*, 2008). MFCs can operate electrical systems and wireless sensors that require low power to transmit signals to receivers in remote locations (Ieropoulos *et al.*, 2005; Shantaram *et al.*, 2005). With the supply of electrical current, MFCs can generate hydrogen, which is stored for later usage (Holzman, 2005). Donovan *et al.* (2008) demonstrated that a sediment MFC can power a wireless sensor. Ieropoulos *et al.* (2013) designed a stacked ceramic MFC to power a cell phone. An MFC could be placed in large intestine to generate and supply electricity to an implantable medical device (Han *et al.*, 2010).

History of MFC

The earliest concept of MFCs was demonstrated by Potter in 1911. Potter (1911) reported that the metabolism of bacteria and yeast generated measurable electricity. Twenty years later, a similar study was done using several different bacteria by Cohen (1931). Davis and Yarbrough (1962) demonstrated a new design of an MFC that consisted of three chambers: One of the outer chambers housed an electrode in aerobic conditions; the other outer chamber housed another electrode in anaerobic conditions; and the middle chamber served as buffer between the two outer chambers. The studies at that time simply showed that power generation is possible. Stirling *et al.* (1983) demonstrated the effects of redox dyes as a mediator of an MFC to improve power generation. Using mediators, various types of bacteria have been studied, such as *Erwinia dissolven* (Vega and Fernandez, 1987), *Proteus mirabilis* (Thurston *et al.*, 1985), *Streptococcus lactis* (Vega and Fernandez, 1987), and *Desulfovibrio desulfuricans* (Park *et al.*, 1997). Without a mediator, Kim *et al.* (1999) and Pham *et al.* (2003) demonstrated the electricity

generation using *Shewanella putrifaciens* and *Aeromonas hydrophila*, respectively. Reimers *et al.* (2001) demonstrated the feasibility of a MFC with marine sediment. Liu and Logan (2004) introduced a single chamber MFC (SCMFC). They simplified the MFC design by removing a separator (proton exchange membrane) between the anode and cathode cambers, and directly exposing the cathode to air. Using the SCMFC, Liu *et al.* (2005) explored the effects of substrate strength, electrode spacing and composition, and temperature in a batch fed SCMFC.

Several studies have been conducted to improve power generation using an SCMFC with various configurations, and the cathode/anode composition. Aelterman *et al.* (2006) improved power output by stacking six MFCs together. Tender *et al.* (2008) demonstrated that marine sediment can be used as MFC media for a viable power supply and that the MFC can charge a capacitor to be used later for power measurement equipment. Dewan *et al.* (2008) studied the relationship between the anode surface area and the power density. In the past years, the performance of MFCs has improved significantly (An *et al.*, 2016).

Research overview

The electrode design has been the greatest challenge in improving the cost effectiveness and scaling up of an MFC (Rabaey *et al.*, 2009). The electrodes are key MFC components that affect MFC performance and cost. Many researchers are looking into finding and developing new electrode materials to overcome the shortcomings such as high costs of electrode material and inconsistent scalability. Since most of the biological reactions occur on the surface of anode, the anode surface area is the primary parameter to improve the MFC performance (Kumar *et al.*, 2013).

In the MFC design, a large variety of carbon materials and metallic materials, with various configurations and surface areas, have been used for anodes (Wei *et al.*, 2011). Although a multitude of carbon-based anode materials have been investigated, only a few studies have used bamboo charcoal for anodes. Chai *et al.* (2010) used local wood charcoal as electrode materials in the construction of an air-cathode MFC. Bamboo charcoal was used as an anode material to study the effects of Pt loading of the cathode surface on the MFC performance Yang *et al.* (2009). Moqsud *et al.* (2013) carried out a study that compared carbon fiber anodes and bamboo charcoal anode and concluded that bamboo charcoal is an effective anode material. The comparison of tubular bamboo charcoal and tubular graphite showed that bamboo charcoal was a better anode material in terms of the surface roughness, biocompatibility, electron transfer, and total internal resistance (Zhang *et al.*, 2014).

The distance between the cathode and anode influences internal resistance of the MFC; thus it affects the MFC performance. Although there are several studies on the effect of electrode distance (or electrode spacing) on the performance of MFCs, no studies have used the bamboo charcoal anodes in their studies. In the present study, SCMFCs having multiple anode plates (MAP), MAP-SCMFC, were constructed using bamboo charcoal as an anode material. The MAP-SCMFC has four plates of bamboo charcoal as anodes, which were placed in the anode chamber at different distances from the cathode.

Chapter Preview

The factors that affect the MFC performance include but are not limited to: (a) the reactor types and configurations; (b) the electrode materials and structures; (c) the

microorganism species and communities; and (d) the effectiveness of substrates and mediators. The anode material and its configuration directly affect the development of a specific microbial community that is involved in power generation. Anode potential is one of the important factors that determine the availability of electrical energy from the biochemical-reactions catalyzed by EAB (Schroder, 2007). In most cases, the material used for the anode is cheaper than that of cathode.

In designing an MFC, the space between the electrodes should be minimized, realizing that the spacing determines the volume and consequently the volumetric power density (Vogl *et al.*, 2016). More importantly, the electrode spacing significantly affects internal resistance of MFCs: i.e., the larger the spacing between the electrodes, the larger the Ohmic losses. Therefore, additional care must be taken when determining the space between the anode and cathode. In a study by Moon *et al.* (2015), the power generation decreased when the anode (graphite felt) was placed very close to the cathode (carbon cloth) or far from the cathode. Their study yielded the maximum power density of 400 mW/m^2 at a distance of 6 mm between the anode and the cathode. The internal resistance decreased at a cathode-to-anode distance of 3 mm and the time-to-peak was shorter at a distance of 9 mm (Moon *et al.*, 2015). Kazemi *et al.* (2016) used flat-plate MFCs with graphite felt anode to evaluate the effect of electrode spacing on oxygen crossover. Using the Up-Flow Constructed Wetland-Microbial Fuel Cell having activated carbon electrodes, Oon *et al.* (2016) studied the electrode spacing on the efficiencies of wastewater treatment and electricity generation. They showed that the MFC with larger distances between the electrodes performed better than that with the electrodes that were placed close together. Oon *et al.* (2016) explained that the reduced efficiency was

attributed to an insufficient fuel supply to the electrodes that were closed together. In the first part of the present study, the performance (in terms of electrode potential and power density) of the MAP-SCMFC was examined as a function of the spacing of the anode plates.

To improve MFC technologies, there are limitations that affect the MFC performance including but not limited to: (a) the rate of substrate degradation (oxidation), (b) the rate of electron transfer from bacteria to the anode, (c) the rate of proton mass transfer in the media, (d) the rate of reduction at the cathode, and (e) the circuit resistance (Liu *et al.*, 2005). Due to these limitations, in many cases, actual power produced by an MFC is not sufficient to be used directly in practical applications. One possible way to increase the power output is to connect several MFCs together, and to store electrical energy into a capacitor or battery through an energy harvester. Then, at a later time, the capacitor or battery can be used to run powered devices. In the second part of this study, electrical energy from the MAP-SCMFCs was harvested and stored in a capacitor and battery with the help of an energy harvester. In this dissertation, the effect of the distance between the cathode and anode on the MAP-SCMFC performance is discussed in Chapter 2, and the harvesting bioenergy from potato wastewater in the MAP-SCMFC and the storing the electrical energy into a capacitor and a battery is discussed in Chapter 3.

Reference

Aelterman, P.; Rabaey, K.; Pham, H. T.; Boon, N.; Verstraete, W. (2006) Continuous Electricity Generation at High Voltages and Currents Using Stacked Microbial Fuel Cells. *Environmental Science & Technology*, 40, 3388-3394.

An, B. M.; Heo, Y.; Maitlo, H. A.; Park, J. Y. (2016) Scaled-up dual anode/cathode microbial fuel cell stack for actual ethanolamine wastewater treatment. *Bioresource Technology*, 210, 68-73.

Chai, L. F.; Chai, L. C.; Suhaimi, N.; Son, R. (2010) Performance of air-cathode microbial fuel cell with wood charcoal as electrodes. *International Food Research Journal*, 17, 6.

Chang, I. S.; Jang, J. K.; Gil, G. C.; Kim, M.; Kim, H. J.; Cho, B. W.; Kim, B. H. (2004) Continuous determination of biochemical oxygen demand using microbial fuel cell type biosensor. *Biosensors and Bioelectronics*, 19, 607-613.

Cohen, B. (1931) The Bacterial Culture as an Electrical Half-cell. *Journal of Bacteriology*, 21, 18-19.

Corbella, C.; Guivernau, M.; Viñas, M.; Puigagut, J. (2015) Operational, design and microbial aspects related to power production with microbial fuel cells implemented in constructed wetlands. *Water Research*, 84, 232-242.

Davis, J. B.; Yarbrough, H. F. (1962) Preliminary Experiments on a Microbial Fuel Cell. *Science*, 137, 615.

Dewan, A.; Beyenal, H.; Lewandowski, Z. (2008) Scaling up Microbial Fuel Cells. *Environmental Science & Technology*, 42, 7643-7648.

Dewan, A.; Donovan, C.; Heo, D.; Beyenal, H. (2010) Evaluating the performance of microbial fuel cells powering electronic devices. *Journal of Power Sources*, 195, 90-96.

Donovan, C.; Dewan, A.; Heo, D.; Beyenal, H. (2008) Batteryless, Wireless Sensor Powered by a Sediment Microbial Fuel Cell. *Environmental Science & Technology*, 42, 8591-8596.

Han, Y. F.; Yu, C. L.; Liu, H. (2010) A microbial fuel cell as power supply for implantable medical devices. *Biosensors & Bioelectronics*, 25, 2156-2160.

Holzman, D. C. (2005) Microbe power! *Environmental Health Perspectives*, 113, A754+.

Ieropoulos, I.; Greenman, J.; Melhuish, C.; Hart, J. (2005) Energy accumulation and improved performance in microbial fuel cells. *Journal of Power Sources*, 145, 253-256.

Ieropoulos, I. A.; Ledezma, P.; Stinchcombe, A.; Papaharalabos, G.; Melhuish, C.; Greenman, J. (2013) Waste to real energy: the first MFC powered mobile phone. *Physical Chemistry Chemical Physics*, 15, 15312-15316.

Kazemi, S.; Mohseni, M.; Fatih, K. (2016) A Systematic Study of Separators in Air-Breathing Flat-Plate Microbial Fuel Cells—Part 1: Structure, Properties, and Performance Correlations. *Energies*, 9.

Kim, H. J.; Hyun, M. S.; Chang, I. S.; Kim, B. H. (1999) A microbial fuel cell type lactate biosensor using a metal-reducing bacterium, Shewanella putrefaciens. *Journal of Microbiology and Biotechnology*, 9.

Kumar, G. G.; Sarathi, V. G. S.; Nahm, K. S. (2013) Recent advances and challenges in the anode architecture and their modifications for the applications of microbial fuel cells. *Biosensors and Bioelectronics*, 43, 461-475.

Liu, H.; Cheng, S. A.; Logan, B. E. (2005) Power generation in fed-batch microbial fuel cells as a function of ionic strength, temperature, and reactor configuration. *Environmental Science & Technology*, 39, 5488-5493.

Liu, H.; Logan, B. E. (2004) Electricity generation using an air-cathode single chamber microbial fuel cell in the presence and absence of a proton exchange membrane. *Environmental Science & Technology*, 38, 4040-4046.

Logan, B. E.; Rabaey, K. (2012) Conversion of Wastes into Bioelectricity and Chemicals by Using Microbial Electrochemical Technologies. *Science*, 337, 686.

Moon, J. M.; Kondaveeti, S.; Lee, T. H.; Song, Y. C.; Min, B. (2015) Minimum interspatial electrode spacing to optimize air-cathode microbial fuel cell operation with a membrane electrode assembly. *Bioelectrochemistry*, 106, Part B, 263-267.

Moqsud, M. A.; Omine, K.; Yasufuku, N.; Hyodo, M.; Nakata, Y. (2013) Microbial fuel cell (MFC) for bioelectricity generation from organic wastes. *Waste Management*, 33, 2465-2469.

Oon, Y.-L.; Ong, S.-A.; Ho, L.-N.; Wong, Y.-S.; Dahalan, F. A.; Oon, Y.-S.; Lehl, H. K.; Thung, W.-E. (2016) Synergistic effect of up-flow constructed wetland and microbial fuel cell for simultaneous wastewater treatment and energy recovery. *Bioresource Technology*, 203, 190-197.

Park, D. H.; Kim, B. H.; Moore, B.; Hill, H. A. O.; Song, M. K.; Rhee, H. W. (1997) Electrode reaction of Desulfovibrio desulfuricans modified with organic conductive compounds. *Biotechnology Techniques*, 11, 145-148.

Pham, C. A.; Jung, S. J.; Phung, N. T.; Lee, J.; Chang, I. S.; Kim, B. H.; Yi, H.; Chun, J. (2003) A novel electrochemically active and Fe(III)-reducing bacterium phylogenetically related to Aeromonas hydrophila, isolated from a microbial fuel cell. *Fems Microbiology Letters*, 223, 129-134.

Potter, M. C. (1911) Electrical Effects Accompanying the Decomposition of Organic Compounds. *Proceedings of the Royal Society of London. Series B, Containing Papers of a Biological Character*, 84, 260.

Rabaey, K.; Angenant, L.; Schroder, U.; Keller, J. (2009) *Bioelectrochemical Systems: From Extracellular Electron Transfer to Biotechnological Application*. IWA Publishing: London.

Reimers, C. E.; Tender, L. M.; Fertig, S.; Wang, W. (2001) Harvesting energy from the marine sediment-water interface. *Environmental Science & Technology*, 35, 192-195.

Schroder, U. (2007) Anodic electron transfer mechanisms in microbial fuel cells and their energy efficiency. *Physical Chemistry Chemical Physics*, 9, 2619-2629.

Shantaram, A.; Beyenal, H.; Veluchamy, R. R. A.; Lewandowski, Z. (2005) Wireless Sensors Powered by Microbial Fuel Cells. *Environmental Science & Technology*, 39, 5037-5042.

Stirling, J. L.; Bennetto, H. P.; Delaney, G. M.; Mason, J. R.; Roller, S. D.; Tanaka, K.; Thurston, C. F. (1983) Microbial fuel cells. *Biochemical Society Transactions*, 11, 451.

Tender, L. M.; Gray, S. A.; Groveman, E.; Lowy, D. A.; Kauffman, P.; Melhado, J.; Tyce, R. C.; Flynn, D.; Petrecca, R.; Dobarro, J. (2008) The first demonstration of a microbial fuel cell as a viable power supply: Powering a meteorological buoy. *Journal of Power Sources*, 179, 571-575.

Thurston, C. F.; Bennetto, H. P.; Delaney, G. M.; Mason, J. R.; Roller, S. D.; Stirling, J. L. (1985) Glucose Metabolism in a Microbial Fuel Cell. Stoichiometry of Product Formation in a Thionine-mediated Proteus vulgaris Fuel Cell and its Relation to Coulombic Yields. *Microbiology*, 131, 1393-1401.

Vega, C. A.; Fernandez, I. (1987) MEDIATING EFFECT OF FERRIC CHELATE COMPOUNDS IN MICROBIAL FUEL-CELLS WITH LACTOBACILLUS-

PLANTARUM, STREPTOCOCCUS-LACTIS, AND ERWINIA DISSOLVENS. *Bioelectrochemistry and Bioenergetics*, 17, 217-222.

Vogl, A.; Bischof, F.; Wichern, M. (2016) Increase life time and performance of Microbial Fuel Cells by limiting excess oxygen to the cathodes. *Biochemical Engineering Journal*, 106, 139-146.

Wei, J.; Liang, P.; Huang, X. (2011) Recent progress in electrodes for microbial fuel cells. *Bioresource Technology*, 102, 9335-9344.

Yang, S.; Jia, B.; Liu, H. (2009) Effects of the Pt loading side and cathode-biofilm on the performance of a membrane-less and single-chamber microbial fuel cell. *Bioresource Technology*, 100, 1197-1202.

Zhang, J.; Li, J.; Ye, D.; Zhu, X.; Liao, Q.; Zhang, B. (2014) Tubular bamboo charcoal for anode in microbial fuel cells. *Journal of Power Sources*, 272, 277-282.

CHAPTER 2

A Single Chamber Microbial Fuel Cell with Multiple Anode Plates made of Conductive Bamboo Charcoal: Effect of Electrode Spacing

Abstract: A single-chamber microbial fuel cell with multiple-anode plates (MAP-SCMFC-A) was constructed. The MAP-SCMFC-A consisted of an anode chamber, a carbon cloth (Pt-coated) cathode, a carbon paper (CP) anode, and four bamboo-charcoal (BC) anode plates. The circuit configurations allowed continuous and simultaneous voltage measurements with five anodes individually or grouped together. The MAP-SCMFC-A was operated in a draw-and-feed mode using acclimated anaerobic sludge as inoculum and potato-processing wastewater as substrate. The largest maximum power density and smallest internal resistance were produced with the anode closest to the cathode, whereas the smallest maximum power density and largest internal resistance was exhibited by the anode farthest from the cathode. When all the anodes (CP and BCs) were connected together, the power output increased more than an order of magnitude, from 45 mW/cm^2 with the CP anode to 504 mW/cm^2 with all anodes together, and the internal resistance decreased from 372 to 118 Ω.

Introduction

Catalyzed by microorganisms, a microbial fuel cell (MFC) produces electricity via direct conversion of reduced chemical compounds. Potential MFC applications include treating wastewater and simultaneously recovering energy from the wastewater (Rabaey and Verstraete, 2005), removal of sulphide (Logan *et al.*, 2006b), generation of hydrogen (Call and Logan, 2008; Logan *et al.*, 2006a), and biosensors (Chang *et al.*, 2005; Di Lorenzo *et al.*, 2009). The use of MFCs as power sources in space shuttles/stations and self-powered robots have been envisioned (Zhao *et al.*, 2010).

Since the beginning of the first MFC, various types of MFCs have been designed and examined, including but not limited to a flat-plate (Min and Logan, 2004), tubular (Rabaey *et al.*, 2005), circulating column (Kargi and Eker, 2009), stackable (Wang and Han, 2009), and loop configuration (Ryu *et al.*, 2013) MFCs. Two-chambered or dual-chamber MFCs (DCMFC) and single-chamber MFCs (SCMFC) are two fundamental types. A DCMFC consists of an anode chamber (with an anode terminal), a cathode chamber (with a cathode terminal), a proton exchange (or a cation specific) membrane, and an external circuit (conductive wire), and it requires microorganisms (biocatalysts), substrate (anolyte), and catholyte. The SCMFC eliminates a cathode chamber and catholyte from the MFC design by directly exposing one side of the cathode to the atmosphere and the other side to the anolyte. An air-cathode allows oxygen in air to contact with protons in the anode chamber to form water at the cathode surface.

Many factors affect the MFC performance, including reactor types and configurations, electrode materials and structures, microorganism communities, substrates, and mediators. Among these factors, the anode material and its configuration

are particularly important in developing MFCs, as they directly affect the development of a specific microbial community that is involved in power generation. The anode serves as receptors of the electrons liberated by electrochemically active bacteria (EAB) from substrate molecules (Zhao *et al.*, 2010) via various electron-transfer mechanisms (Di Lorenzo *et al.*, 2010). Anode potential is one of the important factors that determine the availability of electrical energy from the biochemical-reactions catalyzed by EAB (Schroder, 2007).

Since the first MFC development, different types of graphite and carbon materials have been used for anodes, including graphite plate (Mohan *et al.*, 2009), graphite rod (Liu *et al.*, 2004), graphite granules (Ryu *et al.*, 2013), woven graphite (Park and Zeikus, 2002), graphite felt (Chaudhuri and Lovley, 2003; Kim *et al.*, 2004; Kim *et al.*, 2002), graphite fiber brush (Ahn and Logan, 2010; Logan *et al.*, 2007), reticulated vitreous carbon (Menicucci *et al.*, 2005), carbon cloth (Ishii *et al.*, 2008; Wang *et al.*, 2008; Yuan *et al.*, 2010), carbon paper (Kim *et al.*, 2007; Lu *et al.*, 2009; Min *et al.*, 2005a; Min *et al.*, 2005b; Min and Logan, 2004; Oh and Logan, 2005), wood charcoal granules (Li Fen *et al.*, 2009), bamboo charcoal (Moqsud *et al.*, 2013; Yang *et al.*, 2009; Zhang *et al.*, 2014), and modified materials such as polypyrrole-coated carbon (Yuan, 2008), ammonia-treated carbon cloth (Cheng and Logan, 2007), carbon felts doped with quinone derivatives (Adachi *et al.*, 2008), graphite incorporated with manganese ion (Park and Zeikus, 2002), graphite coated with tungsten carbide (Rosenbaum *et al.*, 2006), carbon paper with coating of vapor-deposited iron oxide (Kim *et al.*, 2005), and gold-sputtered carbon paper (Sun *et al.*, 2010). Although carbon-based materials are commonly used in the MFC studies, several researchers examined non-carbon materials such as copper

(Kargi and Eker, 2009), stainless steel (Dumas *et al.*, 2007), gold (Richter *et al.*, 2008), and titanium (ter Heijne *et al.*, 2008).

The power output from an MFC has been shown to increase with the decreasing distance between the anode and cathode as a result of a decrease in internal resistance (Liu *et al.*, 2005a; Sangeetha and Muthukumar, 2013). When the cathode and anode are too close in an air-cathode SCMFC, however, the power output decreases because oxygen molecules diffuse through the cathode membrane into the anode chamber, inhibiting the growth of EAB (strict anaerobes) that are responsible for electricity generation. Liu *et al.* (2005a) operated an air-cathode SCMFC by changing the distance between the cathode and anode. They found that decreasing electrode distance from 4 cm to 2 cm resulted in an increase of the power density from 720 to 1,210 mW/m^2. In a continued study by Cheng *et al.* (2006), when the electrode distance was decreased from 2 to 1 cm, the maximum power density decreased from 811 mW/m^2 to 423 mW/m^2 although the internal resistance decreased from 35 to 16 Ω. However, the maximum power density increased to 1,540 mW/m^2 when the MFC with 1-cm electrode spacing was operated in a continuous flow (through the anode toward the cathode) mode. Lanas *et al.* (2014) developed three multiple carbon brush anode SCMFCs and demonstrated that changing the distance of the anode to the cathode from 12 mm to 4 mm significantly increased the power density. Ghangrekar and Shinde (2007) studied the effect of electrode distance on electricity production in a membrane-less microbial fuel cell made with graphite electrodes.

This study focused on electrode spacing in an air-cathode SCMFC. An MFC that contains multiple anode plates (MAP) made of conductive bamboo-charcoal (BC) was

constructed, and its performance (electrode potential and power density) was evaluated as a function of electrode spacing. A schematic of the MAP-SCMFC-A system is shown in Figure1. The characteristics of the MAP-SCMFC-A are that (*i*) the MAP design allows continuous and simultaneous voltage measurement at multiple anode locations, and *ii*) external circuit schemes allow the evaluation of all BC anodes and a carbon paper (CP) anode individually (using the CP anode as a control) or all anodes together, without moving the electrodes.

Bamboo is a fast growing plant. During its growth, it sequesters CO_2 rapidly from the atmosphere and stabilizes it in a solid form. Bamboo-charcoal can be easily manufactured at low cost and minimal carbon footprint, and safely disposed of or reused after its lifetime, as it is a natural material.

Materials and Methods

MAP-SCMFC Construction

A body of the MAP-SCMFC-A was constructed using acrylic sheets (Figure 1). The MFC has outside dimensions of 12.7-cm long, 8.9-cm wide, and 10.8-cm tall, and a working volume of 500 mL. On one end, a circular opening (3-cm diameter) was made to expose a cathode to the atmosphere. The cathode made of single-sided 10% Pt-coated carbon cloth (Fuel Cell Earth, Stoneham, MA) and having an effective surface area of 6.7 cm^2 was connected to a platinum (Pt) wire. The MFC has a carbon paper (CP) anode (Toray Industries, Inc., Tokyo, Japan) on the other end, and four additional anodes made of conductive bamboo-charcoal (BC) plates (Mt Meru Pte Ltd., Singapore) inside the fuel cell chamber. Each BC plate had an estimated total geometric surface area of 85.2 cm^2 (7.62-cm long, 4.57-cm wide, and 0.64-cm thick), not considering surface roughness of

the plate. The BC anodes are identified by the distances measured from the cathode; i.e., BC1, BC2, BC3, and BC4 are located at 9, 7, 5, and 3-cm from the cathode, respectively (Figure 2). A small hole was drilled in the bottom of each BC plate, and a platinum wire was inserted in the hole and glued in place. Four holes were drilled on the bottom of the MFC, through which the platinum wires connected to the anode plates were extruded out of the bottom of the MFC. This independent wiring system permitted connection of the BC anode plates individually or grouped together. Two holes were tapped on the top of the MFC to allow for removal of a spent medium solution and addition of a fresh feed solution.

Substrate and Inoculum Sources

The substrate (fuel) used in this study was made from concentrated potato-processing wastewater obtained from a local food processing plant in Idaho. The organic strength of the wastewater was measured in terms of 5-day biochemical oxygen demand (BOD_5). To prepare a desired strength of substrate feed solution, the concentrated potato wastewater was diluted with deionized water to ensure that the feed solution had a BOD_5 of approximately 700 mg/L. This solution was then buffered to pH 7 using a phosphate buffer. The solution was transferred into 250-mL bottles and autoclaved at 121°C for 20 minutes. After sterilization, the bottles containing the medium solution were securely tightened, sealed, and stored in a refrigerator at 4°C until used.

Anaerobic sludge, a source of original microbial culture, was collected from an anaerobic digester at the Water Pollution Control Plant in the city of Pocatello, Idaho. The anaerobic mixed bacterial community was acclimated in sterilized potato wastewater (300 –700 mg/L BOD_5) in SCMFCs for more than 3 years by feeding fresh sterilized

potato wastewater every two weeks. The inoculum used in this study was bacterial culture collected after 3 years of acclimation.

MFC operation and measurement

To commence the MFC run, the reactor was filled with the sterilized potato-processing wastewater and 20 mL of inoculum. The fuel cell was maintained in an incubator at 32°C and operated in a draw-and-feed mode (cycle). The inoculation and draw-and-feed procedures were carried out inside an inflatable glove chamber filled with nitrogen (N_2) gas. The 5-day biochemical oxygen demand was used as a measure of organic contents in the feed and spent medium solutions. The collected samples were temporarily stored in a refrigerator at 4^oC for later BOD_5 analysis. The BOD_5 test was performed according to Jackson (1993).

The voltage produced by the MFC was continuously logged using a Data Acquisition System (DAS). The DAS consists of a desktop computer equipped with a Data Acquisition board (PCI-6024E, National Instrument, Austin, Texas), virtual instrumentation (LabView, version 8.0), and an external connection block (SCB-6024E, National Instrument). The voltage difference V (volts) between the ends of the resistance R (Ω) was converted to current I (A) using the Ohm's law, $I = V/R$, and to power P (W) using the formula, $P = V^2/R$. The maximum power was determined by varying the external resistance R from 20 to 1,200 Ω. Consistent with other researchers, the units of current and power were converted to mA and mW, respectively. The power density normalized to cathode area (mW/m^2) was calculated by dividing the power (mW) by the projected surface area of the cathode (m^2). The power density normalized to the medium volume (mW/m^3) was calculated by dividing the power (mW) by the projected volume of

the medium contained in the fuel cell chamber (m^3). The same convention was applied to the expression of the current densities.

Maximum Power and Internal Resistance Calculations

As the internal resistance and the load resistance are in series to the potential produced in the MFC, the external and internal resistances act as voltage dividers. When both resistances are equal, the resisters effectively divide the supply voltage (total voltage that the MFC is capable of producing) in half. When the load resistance equals the internal resistance, the maximum power results (Nilsson, 1983). In this study, the maximum power was determined by measuring the voltage V with varying the external resistance R. The maximum power is given as

$$P_{max} = V_{max}^2/R_{max} \quad (1)$$

where P_{max} is the maximum power (W), and V_{max} and R_{max} are the voltage produced (V) and the external resistance (Ω), respectively, at the maximum power. Because the external load resisters have discrete resistance values, the largest power computed using $P = V^2/R$ is not necessarily the maximum power; P_{max} can occur between the load resister values used. To find the maximum power in a consistent way, the following method was developed and used. First, current I (A) and power P (W) were calculated using the measured voltage values and the corresponding resistances. Then, the values of voltage and power were plotted against the corresponding current values. In the voltage vs. current plot, a linear relationship existed in the current region where the maximum power occurred; thus,

$$V(I) = a \cdot I + b \quad (2)$$

and

$$V_{max} = a \cdot I_{max} + b \quad (3)$$

where V(I) is voltage as a function of current I, and a and b are the coefficients, which can be determined by a linear least squares fit. Furthermore, because the P vs. I curve followed a quadratic pattern,

$$P(I) = c \cdot I^2 + d \cdot I + e \quad (4)$$

where P(I) is the power as a function of current I, and *c*, *d*, and *e* are the coefficients. These coefficients can be determined by the least squares fit. Accordingly,

$$P_{max} = c \cdot I_{max}^2 + d \cdot I_{max} + e \quad (5)$$

Next, the maximum power was obtained by differentiating Eq. (4), and setting P(I)'= 0:

$$P(I)' = 2\, c \cdot I_{max} + d = 0 \quad (6)$$

Solving Eq. 6 for I_{max} gives

$$I_{max} = - d / 2c \quad (7)$$

where I_{max} is the current at the maximum power. Substituting Eq. (7) into Eq. (5) yields maximum power equation:

$$P_{max} = c \cdot (- d / 2c)^2 + d \cdot (- d / 2c) + e \quad (8)$$

Similarly, substituting Eq. (7) into Eq. (3) gives

$$V_{max} = a \cdot I_{max} + b = b - a(d/2c) \quad (9)$$

Finally, the internal resistance is obtained by Ohm's law:

$$R_{internal} = V_{max} / I_{max} = (a \cdot d - 2b \cdot c)/d \quad (10)$$

where $R_{internal}$ is the internal resistance (ohm). This method offers an advantage of minimizing a human bias in finding the maximum power output and internal resistance values from the MFC experimental data.

Results and Discussion

MAP-SCMFC Startup and Operation

The inoculum used in this study was bacterial mixed culture collected after 3 years of acclimation in a SCMFC with a CP anode. It has been shown that an MFC enhances the growth of EAB through a natural selection system. Our previous study using the same inoculum and potato-processing wastewater indicated that the bacterial communities in the MFC differed dramatically from those of the anaerobic domestic sludge and potato wastewater inoculum. Using the 16S ribosomal DNA sequencing technique, the same study showed that microbial species detected on the anode were predominantly within the phyla of *Proteobacteria*, *Firmicutes*, and *Bacteroidetes* (Li *et al.*, 2014).

The MAP-SCMFC-A was inoculated for 12 days. The maximum potential during the inoculation period occurred after 4 days (First cycle in Figure 2) for all bamboo charcoal anodes. However, the carbon paper reached its maximum potential after 2 days. Hutchinson *et al.* (2011) observed that when the anode size was reduced, specifically for brush anodes, the startup time for the MFC increased. In our experiment, the startup time for the carbon paper decreased as compared to bamboo charcoal anodes. The effective surface area of carbon paper is 12 times smaller than the bamboo charcoal anode. At the end of the inoculation cycle (second cycle), new substrate was added but no spent substrate was removed. During this cycle the peak potential was reached within 31

hours. When the cycle ended, the MAP-SCMFC-A ended with a higher potential than when it started. A similar trend occurred during the third cycle. The first draw-and-feed cycle was performed on the fourth cycle, i.e., spent substrate removed and new substrate added. During the fourth cycle, the peak was sustained 20 hours longer than the previous cycle. The peak voltage during the fifth cycle was sustained for the same number of hours as in the fourth cycle. At this point, the MAP-SCMFC-A was considered to be fully inoculated and past the developmental phase in terms of collecting biofilm on the anode surface. Voltage was measured across a 1kΩ resistor. The voltages for the first five cycles (1,100 hours) are shown in Figure 2.

In the later cycles (6th cycle and later), the rise and fall of the voltage occurred in a reproducible pattern. Typically, the voltage reached a peak that continued for approximately 84 hours (Figure 3). Among all the anodes, the smallest voltage peak was produced with the CP and the voltage declined most quickly. The order of maximum voltage was 0.288 V with the CP, 0.303 V with the BC1 and BC2, 0.308 V with the BC3, and 0.313 V with the BC4. In a comparison of the BC anodes, voltage reached the highest peak but declined most rapidly with the BC4, whereas voltage reached the lowest peak but decreased at the slowest rate with the BC1. The voltage profiles exhibited by the BC2 and BC3 fell between those of the BC1 and BC4.

The air-cathode MFC with a CP anode is considered the control MAP-SCMFC-A configuration. At the CP anode, the voltage increased to the largest peak rapidly, soon after the MFC was inoculated but it declined quickly. In the following cycles, however, the voltage was lowest at the CP anode. Among the BC anodes, the voltage reached the largest peak with the BC4 anode but decreased at the fastest rate. This phenomenon may

be because the diffusion of oxygen is more prominent at the BC4 anode since it is closest to the air-cathode. As the substrate concentration decreases, oxygen intrusion into the anaerobic chamber is inevitable. Although most of the intruded oxygen molecules were likely scavenged by facultative bacteria grown on/near the cathode membrane, they could inhibit the growth of strict anaerobes responsible for electricity generation (Li *et al.*, 2014). The oxygen intrusion resulted in low Coulombic Efficiency (Lu *et al.*, 2009), and was considered the main disadvantage of air-cathode SCMFCs (Liu and Logan, 2004). With the BC1 anode that is located farthest from the cathode, the voltage reached the lowest peak but declined at the slowest rate. On the other hand, the CP anode exhibited a rapid decline in potential similar to BC4 even though it is the furthest anode from the cathode. This could be due to CP anode being 12 times smaller than the BC anodes. It is also possible that the BC anodes were able to utilize the substrate faster due to larger amount of bacteria attachment, thus starving CP anode from unspent substrate.

Maximum Power Generation: Anodes in Series, Electrode Distance, and Internal Resistance

With varying resistance, voltage was monitored at the CP, BC1, and BC4 anodes individually, and all anodes grouped together. Table 1 presents a summary of the comparison. The coefficient values (a, b, c, and d) determined by the least square fit are presented in Table 2. When the voltage was monitored with the individual anodes (Figure 4), the control CP anode yielded the maximum power density of 45 mW/m^2 with an internal resistance of 372 Ω (Figure 5). In a comparison between the BC1 and BC4 (Figure 6), a larger power density was produced with the BC4. The maximum power densities with the BC1 and BC4 anodes were 125 and 168 mW/m^2, respectively, with the corresponding internal resistances of 158 and 141 Ω, respectively. An increase of the

anode distance of 6 cm (from 3 cm to 9 cm measured from the cathode) resulted in an increase in internal resistance of 17 Ω (from 141 to 158 Ω), giving a resistance per distance of 2.83 Ω /cm. The same distance also decreased the power generation by 43 mW/m^2 (from 168 mW/m^2 to 125 mW/m^2), giving a power per distance of 7.17 mW/m^2cm. Liu *et al.* (2005b) observed the maximum power density increased when the electrode distance was decreased. When all the anodes (a CP and four BCs) were connected together (Figure 7), the MFC yielded the maximum power density of 504 mW/m^2 (Figure 8) and the smallest internal resistance of 118 Ω. Jiang and Li (2009) demonstrated that when they inserted four graphite rods into the same granular activated carbon anode bed, the internal resistance decreased. One interesting thing to note is, unlike in our study, Jiang and Li (2009) observed a decrease in total power output by a factor of four when they used four graphite rods as compared to only one graphite rod. When we connected all anodes in series, the maximum power produced increased by a factor of 11.2 with respect to CP and increased by a factor of 3 with respect to BC4. The Coulombic efficiency was calculated to be 19 % assuming a BOD_5 to COD ratio of 0.8.

Conclusions

A single-chamber microbial fuel cell with multiple-anode plates (MAP- SCMFC-A) was constructed to examine the effects of the electrode spacing on the power output and internal resistance. The MAP-SCMFC's circuit configuration allowed the continuous and simultaneous voltage measurements with the five anodes (CP, BC1, BC2, BC3, and BC4), individually or together.

In a stable MAP-SCMFC-A, the voltage reached the smallest maximum peak and declined most quickly at the CP anode. In a comparison of the BC anodes, the voltage

reached the highest peak but declined most rapidly with the BC4 anode that was located closest to the cathode, whereas the voltage reached the lowest peak but decreased at a slowest rate at the BC1 anode located farthest from the cathode. The order of peak voltages measured with the individual anodes (identified by the distance measured from the cathode) are 0.288 V at the CP (12.7 cm), 0.303 V at the BC1 (9 cm) and BC2 (7 cm), 0.308 V at the BC3 (5 cm), and 0.313 V at the BC4 (3 cm). The largest maximum power density (168 mW/cm^2) and smallest internal resistance (141Ω) were produced with the BC4 anode, and the smallest maximum power density (125 mW/cm^2) and largest internal resistance (158 Ω) with the BC1. The increase in the internal resistance was estimated to be 2.83 Ω/cm of the increase of anode distance from the cathode.

The power output increased more than an order of magnitude, from 45 mW/cm^2 with the CP control anode to 504 mW/cm^2 with all the anodes connected together, and the internal resistance decreased from 372 Ω with the CP anode to 118 Ω with all the anodes grouped together. The result suggests that the optimum power can be obtained when the MFC is run with all the anodes grouped together and that, the MAP-SCMFC-A has a potential to generate much larger power than that generated in this study, by increasing the number of the BC plates.

References

Adachi, M.; Shimomura, T.; Komatsu, M.; Yakuwa, H.; Miya, A. (2008) A novel mediator-polymer-modified anode for microbial fuel cells. *Chemical Communications*, 2055-2057.

Ahn, Y.; Logan, B. E. (2010) Effectiveness of domestic wastewater treatment using microbial fuel cells at ambient and mesophilic temperatures. *Bioresource Technology*, 101, 469-475.

Call, D.; Logan, B. E. (2008) Hydrogen Production in a Single Chamber Microbial Electrolysis Cell Lacking a Membrane. *Environmental Science & Technology*, 42, 3401-3406.

Chang, I. S.; Moon, H.; Jang, J. K.; Kim, B. H. (2005) Improvement of a microbial fuel cell performance as a BOD sensor using respiratory inhibitors. *Biosensors and Bioelectronics*, 20, 1856-1859.

Chaudhuri, S. K.; Lovley, D. R. (2003) Electricity generation by direct oxidation of glucose in mediatorless microbial fuel cells. *Nat Biotech*, 21, 1229-1232.

Cheng, S.; Liu, H.; Logan, B. E. (2006) Increased Power Generation in a Continuous Flow MFC with Advective Flow through the Porous Anode and Reduced Electrode Spacing. *Environmental Science & Technology*, 40, 2426-2432.

Cheng, S.; Logan, B. E. (2007) Ammonia treatment of carbon cloth anodes to enhance power generation of microbial fuel cells. *Electrochemistry Communications*, 9, 492-496.

Di Lorenzo, M.; Curtis, T. P.; Head, I. M.; Scott, K. (2009) A single-chamber microbial fuel cell as a biosensor for wastewaters. *Water Research*, 43, 3145-3154.

Di Lorenzo, M.; Scott, K.; Curtis, T. P.; Head, I. M. (2010) Effect of increasing anode surface area on the performance of a single chamber microbial fuel cell. *Chemical Engineering Journal*, 156, 40-48.

Dumas, C.; Mollica, A.; Féron, D.; Basséguy, R.; Etcheverry, L.; Bergel, A. (2007) Marine microbial fuel cell: Use of stainless steel electrodes as anode and cathode materials. *Electrochimica Acta*, 53, 468-473.

Ghangrekar, M. M.; Shinde, V. B. (2007) Performance of membrane-less microbial fuel cell treating wastewater and effect of electrode distance and area on electricity production. *Bioresource Technology*, 98, 2879-2885.

Hutchinson, A. J.; Tokash, J. C.; Logan, B. E. (2011) Analysis of carbon fiber brush loading in anodes on startup and performance of microbial fuel cells. *Journal of Power Sources*, 196, 9213-9219.

Ishii, S.; Watanabe, K.; Yabuki, S.; Logan, B. E.; Sekiguchi, Y. (2008) Comparison of electrode reduction activities of Geobacter sulfurreducens and an enriched consortium in an air-cathode microbial fuel cell. *Appl Environ Microbiol*, 74, 7348-7355.

Jackson, G. B. (1993) *Applied Water and Spentwater Chemistry: A Laboratory Manual*. Van Nostrand Reinhold: New York.

Jiang, D.; Li, B. (2009) Granular activated carbon single-chamber microbial fuel cells (GAC-SCMFCs): A design suitable for large-scale wastewater treatment processes. *Biochemical Engineering Journal*, 47, 31-37.

Kargi, F.; Eker, S. (2009) High power generation with simultaneous COD removal using a circulating column microbial fuel cell. *Journal of Chemical Technology & Biotechnology*, 84, 961-965.

Kim, B. H.; Park, H. S.; Kim, H. J.; Kim, G. T.; Chang, I. S.; Lee, J.; Phung, N. T. (2004) Enrichment of microbial community generating electricity using a fuel-cell-type electrochemical cell. *Applied Microbiology and Biotechnology*, 63, 672-681.

Kim, H. J.; Park, H. S.; Hyun, M. S.; Chang, I. S.; Kim, M.; Kim, B. H. (2002) A mediator-less microbial fuel cell using a metal reducing bacterium, Shewanella putrefaciens. *Enzyme and Microbial Technology*, 30, 145-152.

Kim, J.; Min, B.; Logan, B. (2005) Evaluation of procedures to acclimate a microbial fuel cell for electricity production. *Applied Microbiology and Biotechnology*, 68, 23-30.

Kim, J. R.; Jung, S. H.; Regan, J. M.; Logan, B. E. (2007) Electricity generation and microbial community analysis of alcohol powered microbial fuel cells. *Bioresource Technology*, 98, 2568-2577.

Lanas, V.; Ahn, Y.; Logan, B. E. (2014) Effects of carbon brush anode size and loading on microbial fuel cell performance in batch and continuous mode. *Journal of Power Sources*, 247, 228-234.

Li Fen, C.; Lay Ching, C.; Radu, S.; Napis, S. Performance of air-cathode microbial fuel cell with wood charcoal as electrodes. 7-8 Dec. 2009, 59-61.

Li, Z.; Haynes, R.; Sato, E.; Shields, M.; Fujita, Y.; Sato, C. (2014) Microbial community analysis of an air-cathode single chamber microbial fuel cell utilizing potato wastewater. *Water Environmental Research*, 86, 7.

Liu, H.; Cheng, S.; Logan, B. E. (2005a) Power Generation in Fed-Batch Microbial Fuel Cells as a Function of Ionic Strength, Temperature, and Reactor Configuration. *Environmental Science & Technology*, 39, 5488-5493.

Liu, H.; Cheng, S. A.; Logan, B. E. (2005b) Power generation in fed-batch microbial fuel cells as a function of ionic strength, temperature, and reactor configuration. *Environmental Science & Technology*, 39, 5488-5493.

Liu, H.; Logan, B. E. (2004) Electricity generation using an air-cathode single chamber microbial fuel cell in the presence and absence of a proton exchange membrane. *Environmental Science & Technology*, 38, 4040-4046.

Liu, H.; Ramnarayanan, R.; Logan, B. E. (2004) Production of Electricity during Wastewater Treatment Using a Single Chamber Microbial Fuel Cell. *Environmental Science & Technology*, 38, 2281-2285.

Logan, B.; Cheng, S.; Watson, V.; Estadt, G. (2007) Graphite Fiber Brush Anodes for Increased Power Production in Air-Cathode Microbial Fuel Cells. *Environmental Science & Technology*, 41, 3341-3346.

Logan, B. E.; Hamelers, B.; Rozendal, R.; Schroder, U.; Keller, J.; Freguia, S.; Aelterman, P.; Verstraete, W.; Rabaey, K. (2006a) Microbial fuel cells: methodology and technology. *Environ Sci Technol*, 40, 5181-5192.

Logan, B. E.; Hamelers, B.; Rozendal, R.; Schröder, U.; Keller, J.; Freguia, S.; Aelterman, P.; Verstraete, W.; Rabaey, K. (2006b) Microbial Fuel Cells: Methodology and Technology†. *Environmental Science & Technology*, 40, 5181-5192.

Lu, N.; Zhou, S.-g.; Zhuang, L.; Zhang, J.-t.; Ni, J.-r. (2009) Electricity generation from starch processing wastewater using microbial fuel cell technology. *Biochemical Engineering Journal*, 43, 246-251.

Menicucci, J.; Beyenal, H.; Marsili, E.; Veluchamy; Demir, G.; Lewandowski, Z. (2005) Procedure for Determining Maximum Sustainable Power Generated by Microbial Fuel Cells. *Environmental Science & Technology*, 40, 1062-1068.

Min, B.; Cheng, S.; Logan, B. E. (2005a) Electricity generation using membrane and salt bridge microbial fuel cells. *Water Research*, 39, 1675-1686.

Min, B.; Kim, J.; Oh, S.; Regan, J. M.; Logan, B. E. (2005b) Electricity generation from swine wastewater using microbial fuel cells. *Water Research*, 39, 4961-4968.

Min, B.; Logan, B. E. (2004) Continuous Electricity Generation from Domestic Wastewater and Organic Substrates in a Flat Plate Microbial Fuel Cell. *Environmental Science & Technology*, 38, 5809-5814.

Mohan, S. V.; Raghavulu, S. V.; Peri, D.; Sarma, P. N. (2009) Integrated function of microbial fuel cell (MFC) as bio-electrochemical treatment system associated with bioelectricity generation under higher substrate load. *Biosensors and Bioelectronics*, 24, 2021-2027.

Moqsud, M. A.; Omine, K.; Yasufuku, N.; Hyodo, M.; Nakata, Y. (2013) Microbial fuel cell (MFC) for bioelectricity generation from organic wastes. *Waste Management*, 33, 2465-2469.

Nilsson, J. W. (1983) *Electric Circuits*. Addison-Wesley: Massachusetts.

Oh, S.; Logan, B. E. (2005) Hydrogen and electricity production from a food processing wastewater using fermentation and microbial fuel cell technologies. *Water Research*, 39, 4673-4682.

Park, D.; Zeikus, J. (2002) Impact of electrode composition on electricity generation in a single-compartment fuel cell using Shewanella putrefaciens. *Applied Microbiology and Biotechnology*, 59, 58-61.

Rabaey, K.; Clauwaert, P.; Aelterman, P.; Verstraete, W. (2005) Tubular Microbial Fuel Cells for Efficient Electricity Generation. *Environmental Science & Technology*, 39, 8077-8082.

Rabaey, K.; Verstraete, W. (2005) Microbial fuel cells: novel biotechnology for energy generation. *Trends Biotechnol*, 23, 291-298.

Richter, H.; McCarthy, K.; Nevin, K. P.; Johnson, J. P.; Rotello, V. M.; Lovley, D. R. (2008) Electricity Generation by Geobacter sulfurreducens Attached to Gold Electrodes. *Langmuir*, 24, 4376-4379.

Rosenbaum, M.; Zhao, F.; Schröder, U.; Scholz, F. (2006) Interfacing Electrocatalysis and Biocatalysis with Tungsten Carbide: A High-Performance, Noble-Metal-Free Microbial Fuel Cell. *Angewandte Chemie International Edition*, 45, 6658-6661.

Ryu, J. H.; Lee, H. L.; Lee, Y. P.; Kim, T. S.; Kim, M. K.; Anh, D. T. N.; Tran, H. T.; Ahn, D. H. (2013) Simultaneous carbon and nitrogen removal from piggery wastewater using loop configuration microbial fuel cell. *Process Biochemistry*, 48, 1080-1085.

Sangeetha, T.; Muthukumar, M. (2013) Influence of electrode material and electrode distance on bioelectricity production from sago-processing wastewater using microbial fuel cell. *Environmental Progress & Sustainable Energy*, 32, 390-395.

Schroder, U. (2007) Anodic electron transfer mechanisms in microbial fuel cells and their energy efficiency. *Physical Chemistry Chemical Physics*, 9, 2619-2629.

Sun, M.; Zhang, F.; Tong, Z.-H.; Sheng, G.-P.; Chen, Y.-Z.; Zhao, Y.; Chen, Y.-P.; Zhou, S.-Y.; Liu, G.; Tian, Y.-C.; Yu, H.-Q. (2010) A gold-sputtered carbon paper as an anode for improved electricity generation from a microbial fuel cell inoculated with Shewanella oneidensis MR-1. *Biosensors and Bioelectronics*, 26, 338-343.

ter Heijne, A.; Hamelers, H. V. M.; Saakes, M.; Buisman, C. J. N. (2008) Performance of non-porous graphite and titanium-based anodes in microbial fuel cells. *Electrochimica Acta*, 53, 5697-5703.

Wang, B.; Han, J.-I. (2009) A single chamber stackable microbial fuel cell with air cathode. *Biotechnology Letters*, 31, 387-393.

Wang, X.; Feng, Y. J.; Lee, H. (2008) Electricity production from beer brewery wastewater using single chamber microbial fuel cell. *Water Sci Technol*, 57, 1117-1121.

Yang, S.; Jia, B.; Liu, H. (2009) Effects of the Pt loading side and cathode-biofilm on the performance of a membrane-less and single-chamber microbial fuel cell. *Bioresource Technology*, 100, 1197-1202.

Yuan, Y.; Zhou, S.; Zhuang, L. (2010) Polypyrrole/carbon black composite as a novel oxygen reduction catalyst for microbial fuel cells. *Journal of Power Sources*, 195, 3490-3493.

Yuan, Y. K., Sung-Hyun. (2008) Improved Performance of a Microbial Fuel Cell with Polypyrrole/Carbon Black Composite Coated Carbon Paper Anodes. *Bull. Korean Chem. Soc.*, 29, 5.

Zhang, J.; Li, J.; Ye, D.; Zhu, X.; Liao, Q.; Zhang, B. (2014) Tubular bamboo charcoal for anode in microbial fuel cells. *Journal of Power Sources*, 272, 277-282.

Zhao, Y.; Watanabe, K.; Nakamura, R.; Mori, S.; Liu, H.; Ishii, K.; Hashimoto, K. (2010) Three-Dimensional Conductive Nanowire Networks for Maximizing Anode Performance in Microbial Fuel Cells. *Chemistry – A European Journal*, 16, 4982-4985.

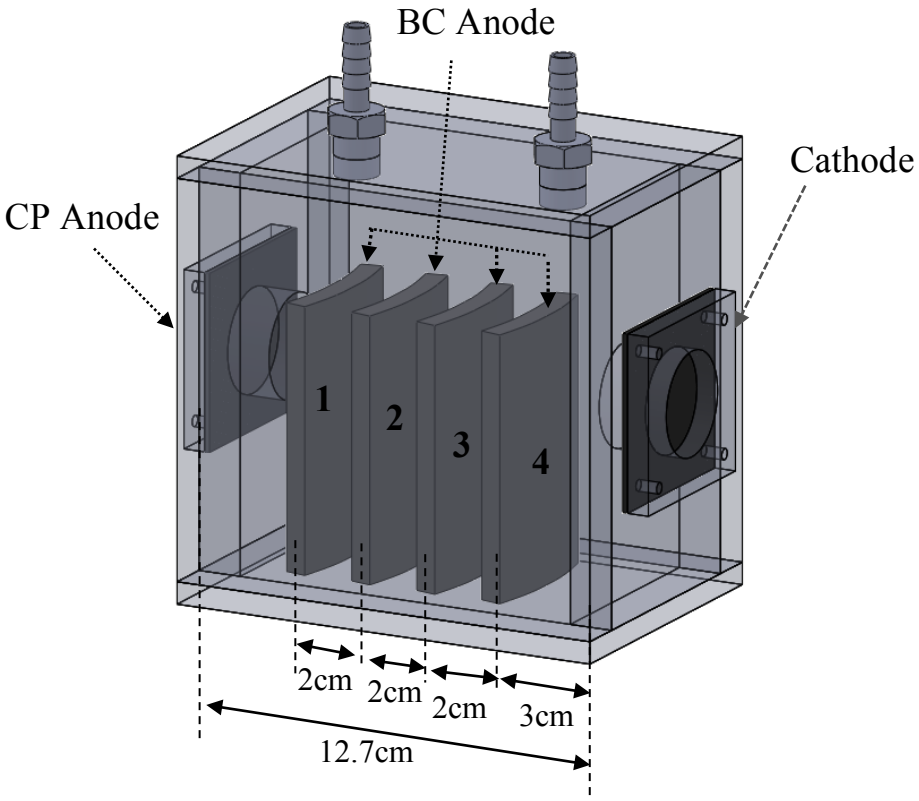

Figure 2-1: Diagram of the air-cathode MAP-SCMFC-A with one carbon paper (CP) anode and four bamboo-charcoal (BC) anode plates and the distance between each anode.

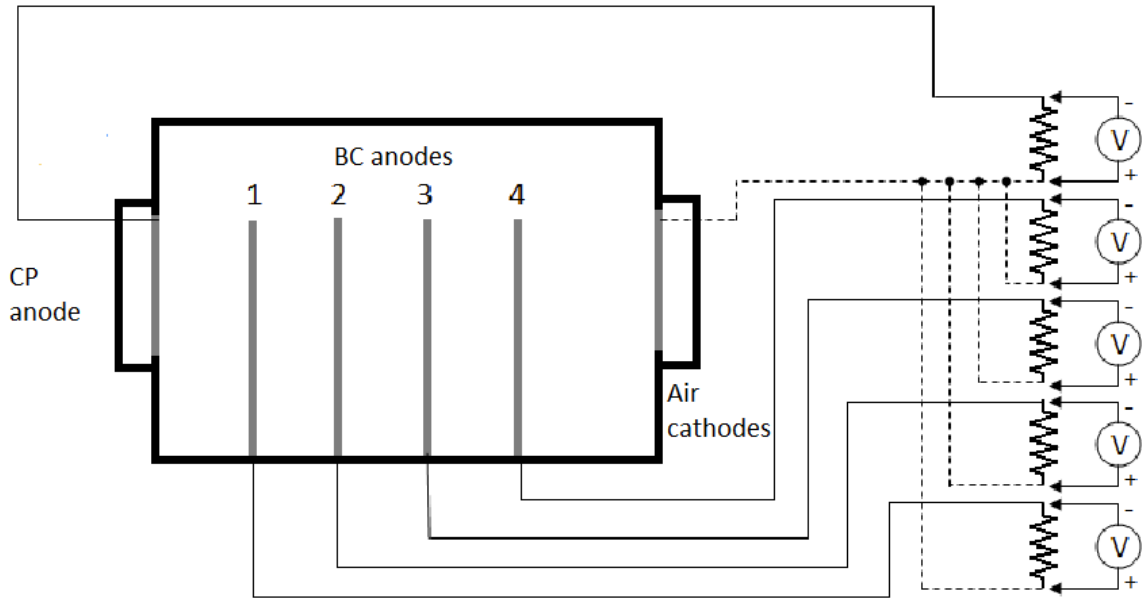

Figure 2-2: The circuit when voltage was measured at individual anodes at external resistance of 1kΩ per circuit.

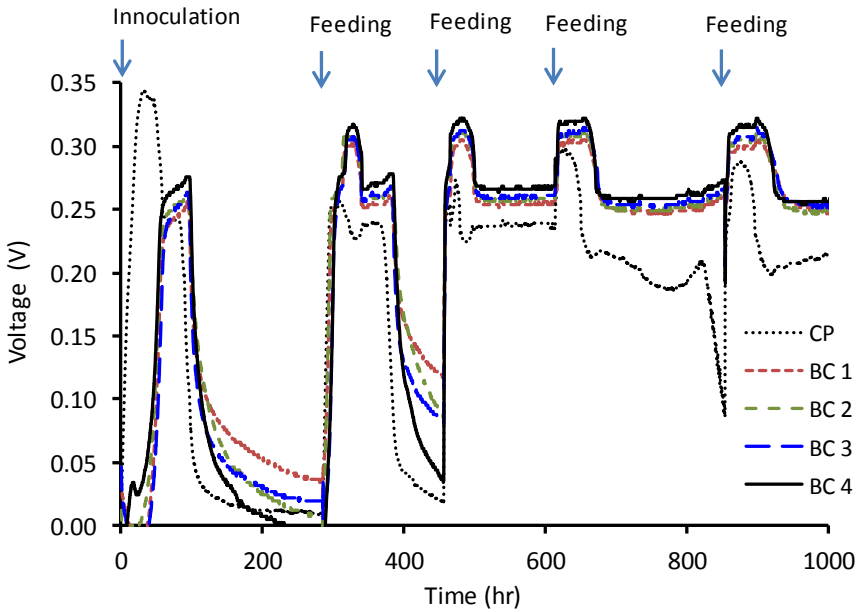

Figure 2-3: Voltage output measured with an external resistance of 1kΩ during the first five cycles. CP = carbon paper anode, BC = bamboo charcoal anode plate; 1 indicates the anode plate closest to CP, 4 indicates the anode plate closest to the cathode and farthest from CP.

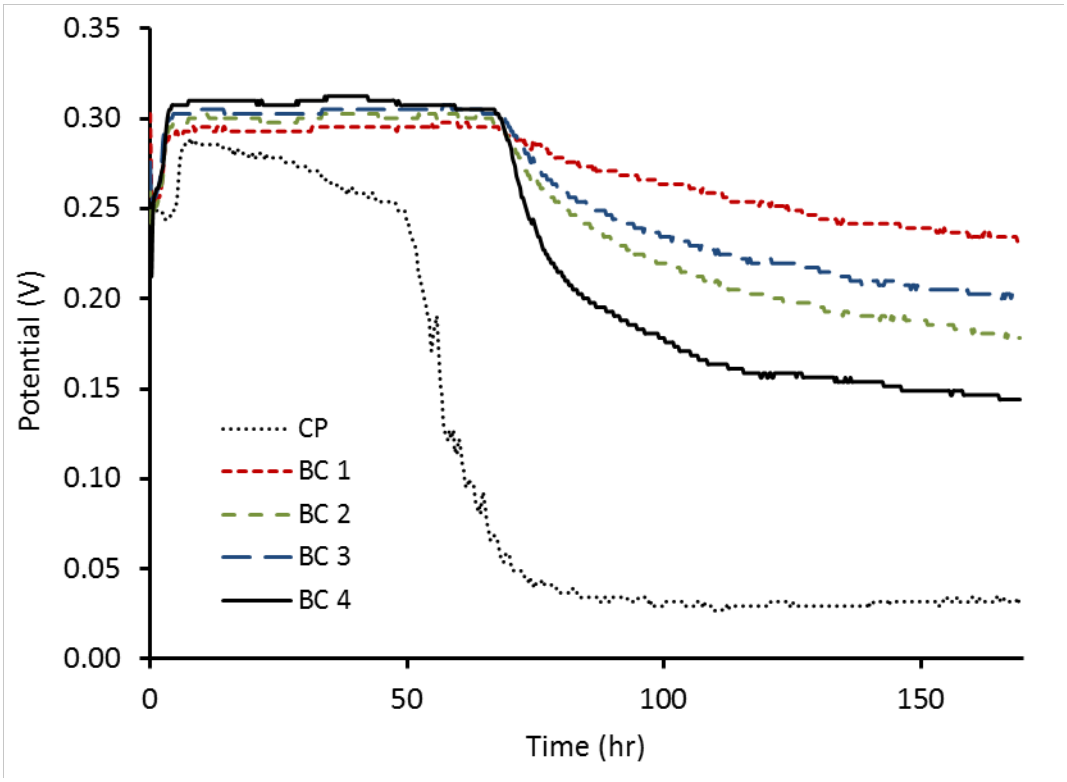

Figure 2-4: Voltage output measured at individual anodes at external resistance of 1kΩ during a stable stage. BC refers to bamboo charcoal plate (anode); 1 indicates the anode plate farthest from the cathode, 4 indicates the anode plate closest to the cathode.

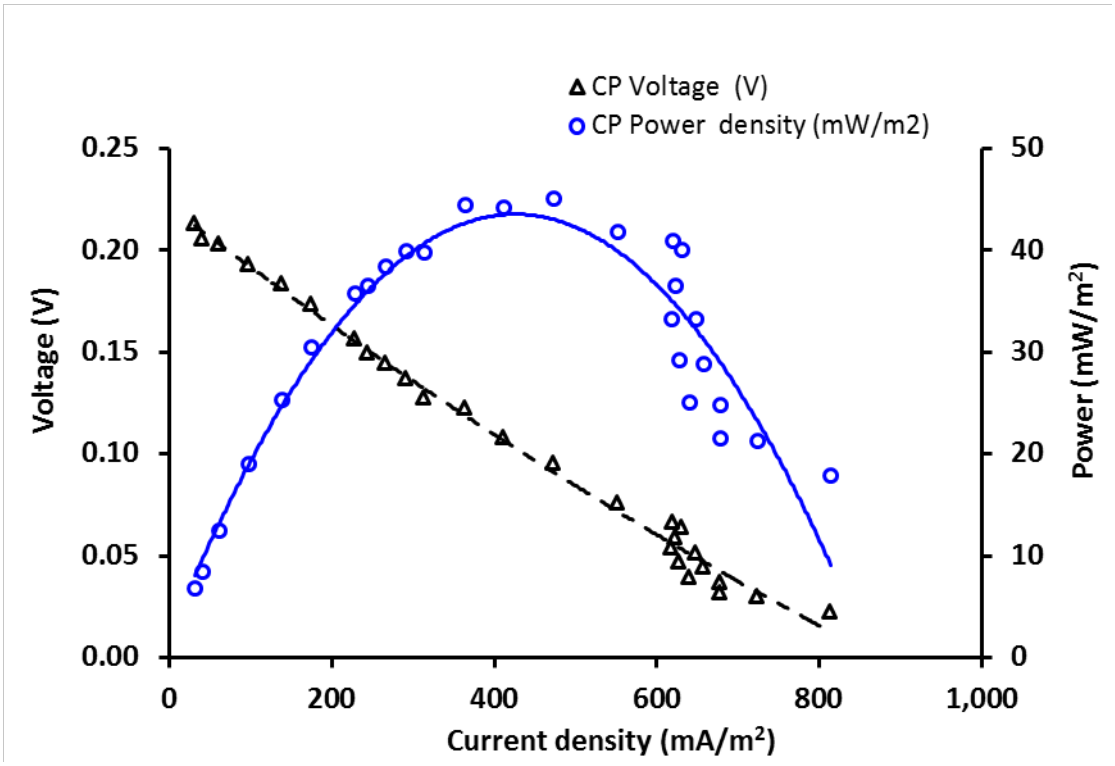

Figure 2-5: Voltage and power generated in the MAP-SCMFC-A with a carbon paper anode when external resistance on the system was changed from 20 to 3000 Ω.

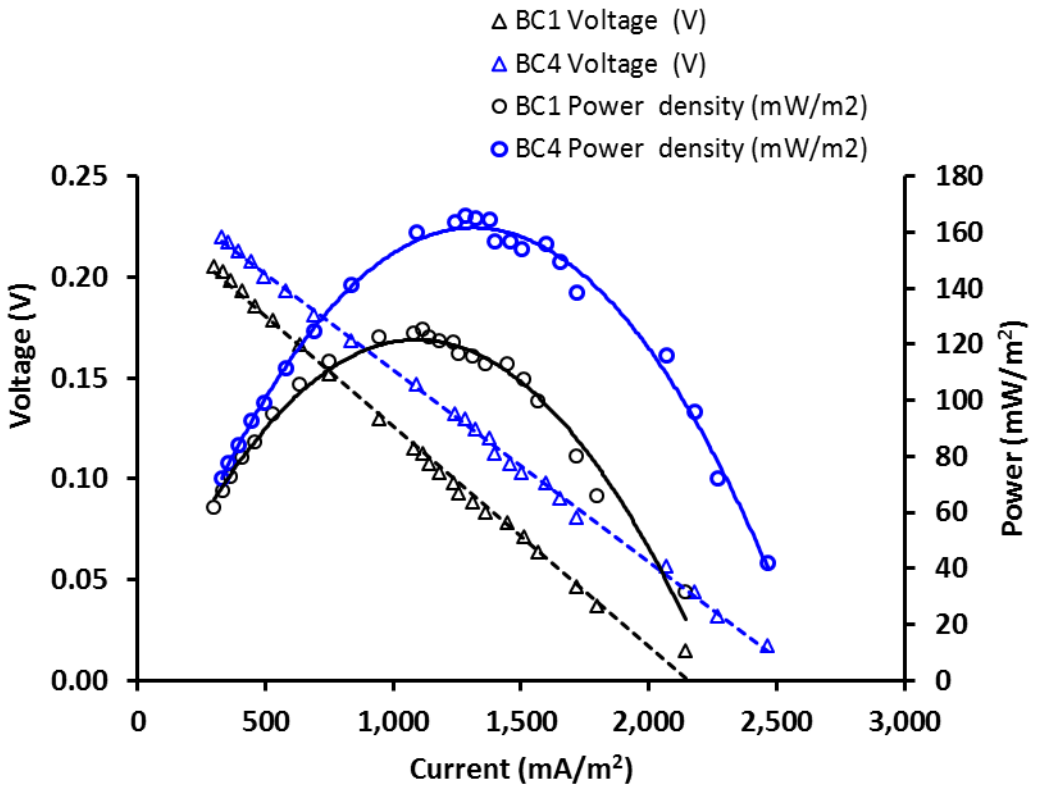

Figure 2-6: Voltage and power generated in the MAP-SCMFC-A at the BC1 anode and the BC4 anode when external resistance on the system was changed from 20 to 1000 Ω. BC refers to bamboo charcoal plate (anode); 1 indicates the anode plate farthest from the cathode, 4 indicates the anode plate closest to the cathode.

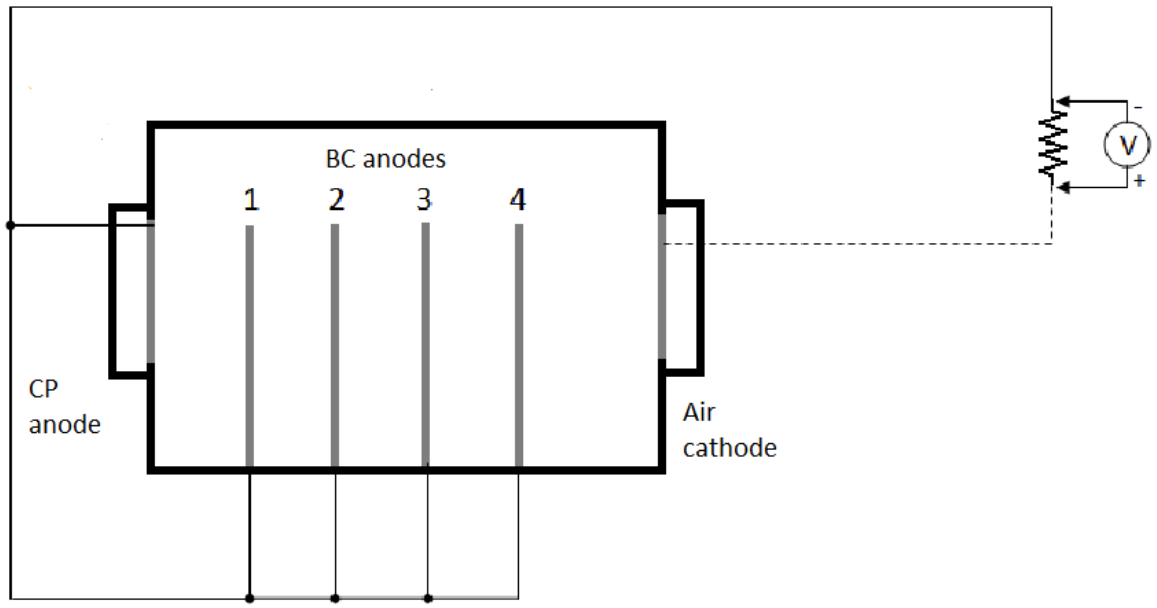

Figure 2-7: The circuit when voltage was measured with all anodes grouped together at external resistance of 1kΩ.

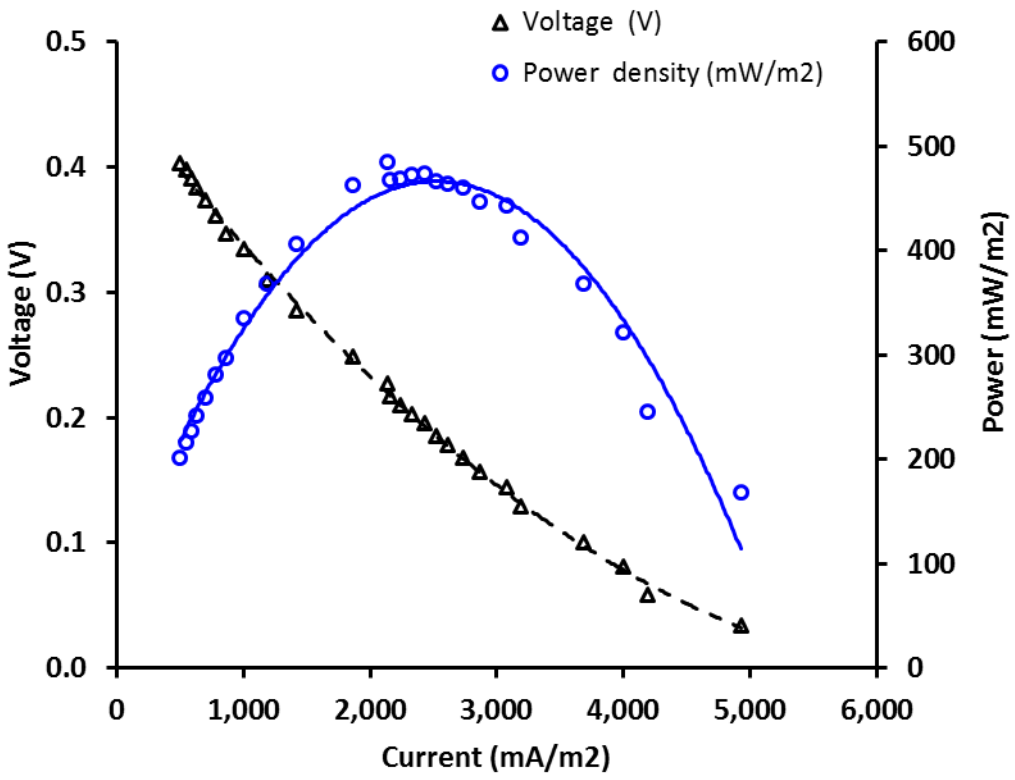

Figure 2-8: Voltage and power generated in the MAP-SCMFC-A with all anodes when external resistance on the system was changed from 20 to 1200 Ω.

Table 2-1: Comparison of MAP-SCMFC-A's performance according to the anodes.

MAP-SCMFC performance parameter		Unit	Carbon Paper	Bamboo Charcoal		CP and all 4 BCs
			CP	BC1	BC4	ALL
Potential	V_{max}	V	0.106	0.116	0.124	0.2
Current	I_{max}	mA	0.285	0.732	0.881	1.691
Power	P_{max}	mW	0.0303	0.084	0.11	0.337
Internal Resistance	R_{max}	Ohm	372	158	140.7	118
Power Density[1]		mW/m^2	45.1	125	168	504
Current Desntiy[1]		mA/m^2	424	1090	1310	2520
Power Density[2]		mW/m^3	60.6	168	220	675
Current Density[2]		mA/m^3	570	1460	1740	3380

[1]based on cathode area (exposed to air)

[2]based on MFC substrate volume

Table 2-2: Coefficient values determined by least square fit.

Coefficient	Carbon Paper	Bamboo Charcoal		CP and all 4 BCs
	CP	BC1	BC4	ALL
a	-0.3839	-0.1629	-0.1418	-0.1329
b	0.2157	0.235	0.2488	0.4243
c	-0.341	-0.1349	-0.1368	-0.0908
d	0.1945	0.1976	0.241	0.3071
Internal resistance, Ohm[1]	373	158	140.7	118

[1]Calculated resistance that yielded maximum power

CHAPTER 3

Harvesting power from bamboo charcoal

Abstract: Two single-chamber microbial fuel cells with multiple-anode plates (MAP-SCMFCs) were used in this study. Each MFC consisted of an anode chamber, containing a carbon paper (CP) anode and four bamboo-charcoal (BC) anode plates. The circuit configurations allowed continuous and simultaneous voltage measurements with five anodes individually or grouped together and with the capability to connect both MFCs in series. An energy harvester was placed in the circuit configuration to harvest and store power in a capacitor and battery. The MAP-SCMFCs were operated in a draw-and-feed mode using acclimated anaerobic sludge as inoculum and potato-processing wastewater as substrate. The highest power produced by the MAP-SCMFCs, when they were placed in series with all the anodes connected together in each of the MFCs (MMFC-AB), was 1328 mW/m^2 with respect to cathode area. The power density with respect to anode area (13 mW/m^2) produced by MMFC-AB configuration was similar to that produced by the MFCs with one BC anode.

Keywords: Microbial Fuel Cell; Bamboo Charcoal Anode; Energy Harvesting; Multiple Anodes; Series Connection

Introduction

Microbial fuel cells (MFCs) represent a particular case of fuel cells in which the direct conversion of chemical into electrical energy is due to the action of biocatalysts (Di Lorenzo *et al.*, 2010). The MFC's anode material and its configuration represent one of the important parameters, as they influence the development of the microbial community involved in the electrochemical bio-reactions (Di Lorenzo *et al.*, 2010). According to the working principle of MFCs, the microbial activity on the anode is essential in liberating electrons from various organics, and the anode potential is one of the determining elements for the collection of energy from the microorganisms (Schroder, 2007). Therefore, the selection of anode material for the construction of an MFC is crucial. Logan *et al.* (2006) stated that the ideal characteristics of anode material include: (a) good electrical conductivity and low resistance; (b) strong biocompatibility; (c) chemical stability and anti-corrosion; (d) large surface area; and (e) appropriate mechanical strength and toughness.

In this study, bamboo charcoal was selected as an anode material because it exhibits the characteristics of an excellent anode material. Zhang *et al.* (2014) conducted a study using tubular bamboo charcoal for anode in microbial fuel cells. A graphite tube anode was also employed in their experiment and the performance of these two anode materials were compared. The results clearly indicated that the bamboo charcoal anode had rougher surface, superior biocompatibility, faster electron transfer, and smaller total internal resistance. Moqsud *et al.* (2013) carried out a study with various electrode materials and concluded that bamboo charcoal is a good, environment friendly anode material.

Charcoal is a stabilized carbon form, and the worldwide applications of the MFC that utilize charcoal may promote a large scale production of charcoal by stabilizing organic carbon into recalcitrant solid charcoal. This can result in reduction of the CO_2 discharge into the atmosphere, and may help mitigate global warming. Furthermore, the price for same amount of charcoal is cheaper than pure carbon or graphite. Therefore, charcoal holds a great promise in reducing the cost and brings the technology into real-world application (Chai *et al.*, 2010). Chai *et al.* (2010) used local wood charcoal as the main component of the electrodes of an air-cathode MFC. The air cathode was built with finely milled charcoal powder and cement plaster as binder, while the anode was made up of a packed bed of charcoal granules. Yang *et al.* (2009) used bamboo charcoal as the anode of a single-chamber MFC, and investigated the effects of Pt loading side on electricity generation of the MFC, the electricity generation in short period and long period operations, the loss of water in anode chamber solution, the diffusion of O_2 into anode chamber, and the functions of cathode-biofilm. High quality charcoal (e.g.,, bamboo charcoal) could have resistance lower than 10 Ω (Yang *et al.*, 2009).

Even selecting an ideal anode material, the power generated in MFCs is limited and not enough to power any high-power-consuming electronic device continuously (Dewan *et al.*, 2010). Some studies have shown that the power of an MFC can be increased by using a multiple electrode system (Jiang *et al.*, 2011; Jiang and Li, 2009; Lanas *et al.*, 2014). Other studies have shown that power can be increased when several MFCs are connected into series(An *et al.*, 2014; Boghani *et al.*, 2014; Choi and Ahn, 2013; Choi and Chae, 2012; Jafary *et al.*, 2013; Oh and Logan, 2007; Rahimnejad *et al.*, 2012; Zhang and Angelidaki, 2012; Zhuang *et al.*, 2012). However, even using multiple

electrode MFCs or MFCs in series, the energy produced may not be enough to operate high- power devices. One solution is to harvest energy from the MFC and store it in capacitor or battery, then use the stored energy as needed to run high-powered devices.

To harvest usable MFC energy, resistors have to be replaced with devices that can capture and store energy and boost voltage for practical usage (Wang *et al.*, 2015). In their study on generating higher power using single or multiple MFCs, Aelterman *et al.* (2006) and Dewan *et al.* (2008) reported that only by building larger MFCs or simply connecting MFCs in series or parallel does not result in larger power production due to the nonlinear nature of MFCs. Therefore, the use of energy harvesting systems or power management systems (PMS) is crucial for MFC scale-up and real-world application (Wang *et al.*, 2015).

Several studies have used sediment MFCs to harvest power employing a power management system (Dewan *et al.*, 2010; Donovan *et al.*, 2008; Donovan *et al.*, 2013; Donovan *et al.*, 2011; Meehan *et al.*, 2011; Shantaram *et al.*, 2005; Tender *et al.*, 2008; Thomas *et al.*, 2013; Zhang *et al.*, 2011). Dewan *et al.* (2010) demonstrated an intermittent energy harvesting approach that allowed the MFC to charge a capacitor and once the capacitor was charged, the energy stored in the capacitor was used to power a sensor. Shantaram *et al.* (2005) charged a capacitor and then used a modified DC-DC converter to boost the potential to power a wireless transmitter, whereas Donovan *et al.* (2008) used a similar system, but added a charge pump (type of DC-DC converter for capacitors) to boost the potential to power a wireless sensor. Donovan *et al.*, 2008), Meehan *et al.* (2011), and Shantaram *et al.* (2005) powered a hydrophone using an MFC along with additional circuitry to boost the MFC output. Thomas *et al.* (2013) used a

transformer based PMS that utilized a Linear Technology (LTC3108) ultra-low-voltage step-up DC-DC converter to power a wireless sensor network. A few studies, like Zhang *et al.* (2012) and Winfield *et al.* (2014), have demonstrated energy harvesting using a PMS on a single-chambered MFC and a rubber MFC made of laboratory gloves, respectively.

In this study, bamboo charcoal was used as an anode in the construction of two single chamber microbial fuel cells (MFCs) that utilized multiple anode plates of conductive charcoal. Our goals were to determine the effectiveness of bamboo charcoal as an anode material by measuring its performance in power generation, and to store power generated by these MFCs in a capacitor and a lithium ion battery via an energy harvester circuit by (1) using the minimal required configuration to charge, and (2) adding additional anodes to decrease charging time. The purpose of charging the capacitor and battery was to store electrical energy so that the energy can be utilized for portable devices such as a flash light, environmental sensor, and cell phone.

Experimental Protocols

MFC Construction

Two MFCs (denoted as MAP-SCMFC-A and MAP-SCMFC-B) were constructed using clear acrylic sheets cut and fastened together to form an outside dimension of 12.7 cm by 8.9 cm by 10.8 cm, see Figure 1. Each MFC contained four plates of bamboo charcoals inside the chamber and one sheet of carbon paper (as anodes) placed on the end of chamber (one side exposed to substrate), and one cathode on the opposite end. In order to expose the cathode to the atmosphere, a circular opening of 3 cm in diameter was drilled in the plate holding in the cathode. Each bamboo charcoal plate (Mt Meru Pte

Ltd., Singapore) had a geometric surface are of 85.2 cm^2 (7.62 cm long, 4.57 cm wide, and 0.64 cm thick), i.e., the projected geometric dimensions and not the surface roughness or porosity of the bamboo charcoal. Each bamboo charcoal was spaced 2 cm from each other with the bamboo charcoal closest to the cathode spaced 3 cm from the cathode. The carbon paper anode (Toray Industries, Inc., Tokyo, Japan) and Pt-coated carbon cloth cathode (Fuel Cell Earth, Stoneham, MA) have an effective area of 6.7 cm^2. With all the anodes and cathode placed inside the MFC, the chamber had a working volume of 500 mL.

In order to connect the bamboo charcoal anodes to the Data Acquisition System (DAS), a hole was drilled on the bottom of each bamboo charcoal, and platinum wire was inserted into and fixed with an adhesive. Four holes were drilled in the bottom plate of the MFC reactor to allow the wires to pass through the plate such that they can be connected externally. Wiring the bamboo charcoal anode in such a way allowed them to be independently connected to the DAS. Lastly, two holes were drilled and tapped on the top of the MFC to allow for two ports for removing old and adding new substrate.

Substrate

The substrate used in this study was made from concentrated potato-processing wastewater obtained from a local food processing plant in Idaho. The substrate was prepared by diluting the concentrated potato wastewater with buffered (pH 7) deionized water. The organic strength of the wastewater was measured in terms of 5 day biochemical oxygen demand (BOD_5). The measured BOD_5 of the feed substrate solution was approximately 700 mg/L. The BOD_5 test was performed according to Jackson (1993). The substrate was autoclaved at 121°C for 20 minutes in 250 mL bottles. The

bottles containing the sterilized substrate solution were securely tightened, sealed, and stored in a refrigerator at 4°C until used (approximately 2-3 weeks). To minimize variation of organic content (measured using BOD_5) of the feed solution, which could occur during the preparation of the feed solution, a large volume was prepared and stored in a refrigerator until used. Autoclaving was necessary to assure that microbes did not utilize the organic substrate during the storage.

Bacterial culture used in this study is originated from an anaerobic digester at the Water Pollution Control Plant in the city of Pocatello, Idaho. The anaerobic mixed bacterial community was acclimated in sterilized potato wastewater (300 –700 mg/L BOD_5) for more than 3 years by feeding fresh sterilized potato wastewater every two weeks to a month.

MFC Operation

For the first two cycles, the MFCs were filled with the sterilized potato-processing wastewater and 20 mL of inoculum. The MFCs were maintained in an incubator at 32°C and all experiment runs were carried out at this temperature. The original inoculum for the MFCs was collected from an anaerobic digester (heated) in the municipal wastewater treatment plant (City of Pocatello, Idaho), therefore, the MFCs were maintained at a similar temperature as the digester during the experiments.

The MFCs were operated in draw-and-feed cycles. During the draw-and-feed cycle, the MFCs were placed inside an inflatable glove chamber and filled with nitrogen (N_2) gas to create an anaerobic environment.

Each anode in both MFC was connected to individual channels on the DAS and the potential produced by each anode was continuously logged with the DAS. The DAS

consisted of a desktop computer equipped with a Data Acquisition board (PCI-6024E, National Instrument, Austin, Texas), an external connection block (SCB-6024E, National Instrument) and controlled by LabView (version 8.0).

A Texas Instruments (BQ25504) Ultra Low Power Boost Converter with Battery Management was used as an Energy Harvester to charge a capacitor or battery. When the energy harvester was being used, the battery voltage and input voltage to the energy harvester were also being logged by the DAS. The capacitor used in the experiment was a NEC/TOKIN, FA 5V, 1.0F. The battery used in the study was an Ultralast 14500/Lithium Phosphate 3.2V.

Analysis and Calculation

The voltage difference E (volts) between the ends of the resistance R (ohms, Ω) was converted to current I (amperes) using the Ohm's law, $I = V/R$, and to power P (W) using the formula, $P = V^2/R$. External resistance in the circuit varied from 20 to 1,200 Ω, and the polarization curves were measured. The specific resistance values for the polarization curves were chosen to cover a wide range of power and to capture the maximum power output. Consistent with other researchers, the units of current and power were converted to mA and mW, respectively. Power output (W) was normalized using the anode area, the cathode area and the MFC volume. The power density normalized to anode area (mW/m^2) was calculated by dividing the power (mW) by the projected geometric surface area of the bamboo charcoal plates (m^2). The power density normalized to cathode area (mW/m^2) was calculated by dividing the power (mW) by the projected surface area of the cathode (m^2). The power density normalized to the substrate volume (mW/m^3) was calculated by dividing the power (mW) by the substrate volume

(m^3) contained in the MFC. The same convention was applied to the expression of the current densities.

Results and Discussion

Inoculation and MFC Runs

The MAP-SCMFC-A constructed using four plates of bamboo charcoal as anodes was inoculated, and then allowed for biofilm growth on the anodes for 290 hrs (12 days). During this period, the peak potential of 0.276V, measured across a 1 kΩ resistor, was noticed at 95 hrs (4 days) (Figure 2a). Lu *et al.* (2009) reported that power generation in an air-cathode MFC with carbon paper anode depends on the attachment and growth of anode biofilm and they expected this to occur in 9 to 10 days. Sangeetha and Muthukumar (2013) observed in their study of the graphite electrode MFC that maximum power production occurred on the 15th day, which may be due to the time taken for acclimatization, enrichment, and growth of bacteria on the anode surface and eventually produced power generation. From Figure 2a, it is observed that it takes three cycles for the MAP-SCMFC-A to become stable, i.e., the changes are considerably larger during these cycles than the remaining cycles.

During the next five cycles, cycle four through cycle eight, the duration of the peak potential increased by 46 hours, Figure 2b. The increase in the duration of peaks shows that during the initial runs, the charcoal anode was still in the developmental phase in terms of collecting biofilm on the anode surface, and by the eighth cycle, the biofilm layer might have fully established on the surface of the anode plates, as indicated by the prolonged peak. Long lasting peaks indicate steady power generation without the constant interference of the MFCs with the draw-and-feed. Charcoal has a large

microscopic surface area with the outer surface being rough and porous. This allows for more bacterial attachment, and could be the reason for the longer lasting peaks. Yang *et al.* (2000) and Tang *et al.* (2007) established a direct link between biofilm attachment and surface roughness of the electrode. It was reported that the increase in polishing level decreased the surface roughness value and the amount of bacterial adhesion, while a rough surface promoted bacterial adhesion and colonization.

To increase the power generation and hence utilize the generated power to charge a device such as capacitor (and later, a battery), a duplicate MFC (MAP-SCMFC-B) was constructed. During the inoculation and bacterial-growth phase, MAP-SCMFC-B showed similar trends of graphs as MAP-SCMFC-A.

The various configurations and the respective power generation for each configuration used in this study are summarized in Table 1. The values in Table 1 correspond to the maximum power point from the power curves when only a single anode (BC4) from MAP-SCMFC-A (denoted as SMFC-A and shown in Figure 3a) and MAP-SCMFC-B (denoted as SMFC-B and shown in Figure 3b) was used, when all anodes were connected together in MAP-SCMFC-A (denoted as MMFC-A and shown in Figure 4a), and when all anodes were connected together in MAP-SCMFC-A and in MAP-SCMFC-B while MAP-SCMFC-A and MAP-SCMFC-B were connected in series (denoted as MMFC-AB and shown in Figure 4b). The differences in potential between MAP-SCMFC-A and MAP-SCMFC-B might have been due to the maturity and acclimation differences between these MFCs because of the different start times. There could also have been a variation in the surface roughness of the bamboo charcoal and maybe some slight variation during the construction of these MFCs. These differences

were also noticeable when multiple anodes were used. From Table 1, we observe that the collective power (MMFC-AB) is more than double the power produced by MMFC-A, which would imply that MMFC-B would have produced a higher power than MMFC-A so that their sum would be 0.89 mW.

From Table 1, as the number of anodes were increased from one to four in MAP-SCMFC-A, the power density with anode area decreased by about 27%. Although the decrease in power density indicates that adding more bamboo charcoals did not maximize the power generation with respect to anode area, it did increase the overall power generated. This power increase was necessary to operate the Energy Harvester, which will be discussed in the next section. In their study on quantifying the relation between the surface area of the current-limiting electrode of a microbial fuel cell (MFC) and the power density generated by the MFC, Dewan *et al.* (2008) concluded that in MFCs power density decreases with increasing surface area of the current-limiting electrode. If we compare the power density (with respect to anode area) when all anodes in each MFCs were connected together and then the MFCs were connected in series, the power density we obtained was similar to the power density from an MFC with one anode. Stacked MFCs will not deliver higher power densities than the individual MFCs, yet they create the possibility to produce an averaged power at more practical voltages and currents (Aelterman *et al.*, 2006). This overall increase in power generation that was observed will be beneficial for energy harvesting.

Previous studies of wood charcoal and bamboo charcoal have been shown to successfully generate power from using these materials as anodes in single chamber microbial fuel cells. Chai *et al.* (2010) studied the performance of wood charcoal in an

air-cathode microbial fuel cell. The MFC was inoculated with brackish water, and it generated the maximum power density of 17.7 mW/m^2 with respect to the surface area of the cathode (200 Ω, 44.33 mA/m^2). The fuel cell voltage reached a stable value of 399 mV after 2 days operation. Yang *et al.* (2009) worked with bamboo charcoal as their anode material in the construction of a single chamber microbial fuel cell. The results show that the maximum power generated by the reactor was 0.144 mW, producing a current of 0.6 mA (400 Ω), when the Pt-loaded side of the cathode was facing the air. Moqsud *et al.* (2013) used bamboo charcoal with iron wire winding as an anode to investigate the influence of different anode materials in bioelectricity generation by MFCs and obtained the maximum power of 400 mW/m^2. In our study, bamboo charcoal was used in the construction and design of a multiple anode system in single chamber MFCs. Yang *et al.* (2009) mentioned that high quality charcoal such as bamboo charcoal could have resistance lower than 10 Ω. The bamboo charcoal used in our study had a resistance range from 10-12 Ω. The resistance of the bamboo charcoal electrode was measured at several locations of each bamboo charcoal plate using a multimeter (Amprobe 38 XR-A). Furthermore, the price for the same amount of charcoal is cheaper than pure carbon or graphite (Chai *et al.*, 2010). Therefore, charcoal holds great promise in reducing the cost and brings the technology into real-world application. Since bamboo is a fast growing plant and due to its ability to rapidly sequester CO_2 from the atmosphere and stabilize it in a solid form, bamboo-charcoal can be easily manufactured at low cost and minimal carbon footprint, and safely disposed of or reused after its lifetime, as it is a natural material.

Energy Harvesting

An Energy harvester (Texas Instruments BQ25504) was used for this study to charge the capacitor and battery. In order for the energy harvester to begin charging, the minimum input voltage of 0.33V (cold start voltage) must be met by the MFC configuration being used. Considering the different configurations in Table 1, we observe that MAP-SCMFC-A alone with either a single anode or multiple anodes is not sufficient to meet the cold-start voltage. However, if SMFC-A and SMFC-B (single anode configurations) were to be placed in series, their sum of 0.37V would be sufficient for the cold-start voltage. This leads to the first phase of the study, which involved using the anode closest to the cathode from each MFC and putting the two MFCs into series (SMFC-AB). This was considered to be the minimum required configuration for charging. The MFCs were connected to the Energy harvester (EH/SMFC-AB) to charge a capacitor. Figure 5 shows the combined potential of the SMFC-AB configuration, and the potential of the capacitor as it is being charged by the EH/SMFC-AB system. The actual series voltage when they were connected was 0.35V at the start of the charge. This voltage is not necessarily the addition of individual MFCs at peak performance (values in Table 1), since the resistance of the system is not necessarily the same as the internal resistance of the MFCs. Nonetheless, the potential was sufficient to meet the cold-start voltage and begin charging the capacitor. The trend of the potential during charging is noticeably different than the expected trend of a batch fed system, e.g. Figure 2b. Instead, the voltage slightly increases in the charging region denoted by I. It is in this region that the cold start is active. Once the capacitor reaches 1.75V, the SMFC-AB configuration potential begins to rapidly increase, as does the charging of the capacitor until the capacitor is fully charged, region II. Hatzell *et al.* (2013) reported a boost in

potential in their stacked single chamber MFCs while charging a capacitor when the MFCs and capacitor were placed in parallel. In our study, a similar phenomenon may be occurring when charging the capacitor, i.e., the MFCs potential increases as it follows the potential of the capacitor. It is in region II (Figure 5) that the boost operation of the Energy Harvester is active and boosts the input. After the capacitor is fully charged, the system exhibits an open circuit and the MFCs are producing their maximum voltage of 0.66V. From Figure 5, it is seen that it took approximately 22 hours to charge the capacitor from 1 volt to the maximum voltage of 3.125.

The second phase of the study involved replacing the capacitor with a Li-Ion rechargeable battery and using the same configuration, i.e. EH/SMFC-AB. A battery is more versatile than a capacitor and is widely used in a range of devices. Rechargeable 3V Lithium batteries (e.g., Energizer CR123A; Tenergy RCR123A; MicroMall CR2/15270; SuperX CR123A/CR2; Watson CR2) are common batteries for toys, lamps, and electronic devices. Once the MFCs were fed, the battery began to charge, as shown in Figure 6. However, after 169 hours of running, the battery's potential had only increased by 59 mV. From Figure 6, it can be observed that the SMFC-AB configuration's potential follows a similar trend as would be expected in a batch fed system unlike the trend seen during capacitor charging. Since the battery has a total charge voltage of 3.125V, the remaining charge voltage of 0.195V (from Figure 6 the current charge voltage was 2.930V, therefore 3.125-2.930) is required to consider the battery to be fully charged. The average rate at which the EH/SMFC-AB system was charging the battery was 0.35mV/hr (59mV/169hours). At that rate it would take roughly 23 days (557 hours) to

completely charge the battery. Therefore, it is critical to increase the power output of the MFCs, which then would charge the battery faster.

To improve the rate of battery charging and to generate more power from the MFCs, all the anodes in the MAP-SCMFC-A were connected together (MMFC-A). With this setup MAP-SCMFC-A produced a maximum potential of 0.227V, Table 1. Since the voltage produced by MAP-SCMFC-A is below the 0.33V threshold, MAP-SCMFC-A alone could not charge the battery. Therefore, the third phase of the study was to determine how effective both MAP-SCMFC-A and MAP-SCMFC-B when connected in series with the Energy Harvester would be at charging a battery. Connecting the two MFCs in parallel would have increased the current, and thus accelerated the rate of charging; however, the parallel setup would not have produced enough voltage to meet the minimum threshold value of 0.33V that is required for charging to occur. When both MAP-SCMFC-A and MAP-SCMFC-B were connected in series with the individual anodes connected together in each MFC (MMFC-AB), they produced a potential of 0.376V, Table 1. When the MFCs were connected to the Energy Harvester (EH/MMFC-AB), the battery was charged from 2.9 V to the maximum voltage of 3.125 V in approximately 130 hours, as shown in Figure 7. The EH/MMFC-AB configuration decreased the duration of battery charging by nearly a factor of 4.3 as compared to the SMFC-AB configuration (a decrease from 23 days to 130 hours). From Figure 7, it is observed that once the battery is fully charged (i.e., when 3.125 V is reached) the Energy Harvester acts like an open circuit and the MFCs produce their maximum potential.

Once the battery was fully charged, a drain test was performed. The drain test was used to determine how much of the battery's total capacity of 600 mAh was charged

by the EH/MMFC-AB system. This was determined from the difference between the battery's voltage prior to charging with the EH/MMFC-AB system and the battery's voltage when it was fully charged by the EH/MMFC-AB system. The capacity rating was determined to be 13 mAh when the battery was charged from 2.87 V to 3.125 V. This output signifies the battery that was charged could be used in smaller devices that operate with low power, e.g. a wifi module (Microchip RN171). The wifi module consumes 40 mA to receive data on a wifi connection; therefore the battery would support data receiving for about 20 minutes.

Conclusions

The highest power produced by the MAP-SCMFCs, when they were placed in series with all the anodes connected together in each of the MAP-SCMFCs (MMFC-AB), was 1328 mW/m^2 with respect to cathode area. The power density with respect to anode area (13 mW/m^2) produced by MMFC-AB configuration was similar to the power density by the MFCs when only one anode was used (SMFC-A or SMFC-B), i.e., relatively constant power production. With respect to charging a battery, the MFCs in series with all anodes connected together reduced the total charging by roughly a factor of 4.3 as opposed to when only one anode from each MAP-SCMFC was selected. The battery was tested to have a capacity rating of 13 mAh (Energy=38 mWh), which signifies the battery we charged could be used in smaller devices that operate with low power.

We can conclude that bamboo charcoal, as an anode, generated sufficient amount of power to charge a capacitor and a battery when an Energy Harvester was used. When the multiple electrode system was implemented, the MAP-SCMFCs were faster in charging, even more when two MAP-SCMFCs with multiple electrode systems were

connected in series. Therefore, we can say that bamboo charcoal is a feasible anode material for MFCs and is adequate in power generation when multiple anode configurations connected in series are implemented.

Reference

Aelterman, P.; Rabaey, K.; Pham, H. T.; Boon, N.; Verstraete, W. (2006) Continuous Electricity Generation at High Voltages and Currents Using Stacked Microbial Fuel Cells. *Environmental Science & Technology*, 40, 3388-3394.

An, J.; Kim, B.; Jang, J. K.; Lee, H.-S.; Chang, I. S. (2014) New architecture for modulization of membraneless and single-chambered microbial fuel cell using a bipolar plate-electrode assembly (BEA). *Biosensors and Bioelectronics*, 59, 28-34.

Boghani, H. C.; Papaharalabos, G.; Michie, I.; Fradler, K. R.; Dinsdale, R. M.; Guwy, A. J.; Ieropoulos, I.; Greenman, J.; Premier, G. C. (2014) Controlling for peak power extraction from microbial fuel cells can increase stack voltage and avoid cell reversal. *Journal of Power Sources*, 269, 363-369.

Chai, L. F.; Chai, L. C.; Suhaimi, N.; Son, R. (2010) Performance of air-cathode microbial fuel cell with wood charcoal as electrodes. *International Food Research Journal*, 17, 6.

Choi, J.; Ahn, Y. (2013) Continuous electricity generation in stacked air cathode microbial fuel cell treating domestic wastewater. *Journal of Environmental Management*, 130, 146-152.

Choi, S.; Chae, J. (2012) An array of microliter-sized microbial fuel cells generating 100 μW of power. *Sensors and Actuators A: Physical*, 177, 10-15.

Dewan, A.; Beyenal, H.; Lewandowski, Z. (2008) Scaling up Microbial Fuel Cells. *Environmental Science & Technology*, 42, 7643-7648.

Dewan, A.; Donovan, C.; Heo, D.; Beyenal, H. (2010) Evaluating the performance of microbial fuel cells powering electronic devices. *Journal of Power Sources*, 195, 90-96.

Di Lorenzo, M.; Scott, K.; Curtis, T. P.; Head, I. M. (2010) Effect of increasing anode surface area on the performance of a single chamber microbial fuel cell. *Chemical Engineering Journal*, 156, 40-48.

Donovan, C.; Dewan, A.; Heo, D.; Beyenal, H. (2008) Batteryless, Wireless Sensor Powered by a Sediment Microbial Fuel Cell. *Environmental Science & Technology*, 42, 8591-8596.

Donovan, C.; Dewan, A.; Heo, D.; Lewandowski, Z.; Beyenal, H. (2013) Sediment microbial fuel cell powering a submersible ultrasonic receiver: New approach to remote monitoring. *Journal of Power Sources*, 233, 79-85.

Donovan, C.; Dewan, A.; Peng, H.; Heo, D.; Beyenal, H. (2011) Power management system for a 2.5 W remote sensor powered by a sediment microbial fuel cell. *Journal of Power Sources*, 196, 1171-1177.

Hatzell, M. C.; Kim, Y.; Logan, B. E. (2013) Powering microbial electrolysis cells by capacitor circuits charged using microbial fuel cell. *Journal of Power Sources*, 229, 198-202.

Jackson, G. B. (1993) *Applied Water and Spentwater Chemistry: A Laboratory Manual*. Van Nostrand Reinhold: New York.

Jafary, T.; Rahimnejad, M.; Ghoreyshi, A. A.; Najafpour, G.; Hghparast, F.; Daud, W. R. W. (2013) Assessment of bioelectricity production in microbial fuel cells through series and parallel connections. *Energy Conversion and Management*, 75, 256-262.

Jiang, D.; Curtis, M.; Troop, E.; Scheible, K.; McGrath, J.; Hu, B.; Suib, S.; Raymond, D.; Li, B. (2011) A pilot-scale study on utilizing multi-anode/cathode microbial fuel cells (MAC MFCs) to enhance the power production in wastewater treatment. *International Journal of Hydrogen Energy*, 36, 876-884.

Jiang, D.; Li, B. (2009) Granular activated carbon single-chamber microbial fuel cells (GAC-SCMFCs): A design suitable for large-scale wastewater treatment processes. *Biochemical Engineering Journal*, 47, 31-37.

Lanas, V.; Ahn, Y.; Logan, B. E. (2014) Effects of carbon brush anode size and loading on microbial fuel cell performance in batch and continuous mode. *Journal of Power Sources*, 247, 228-234.

Logan, B. E.; Hamelers, B.; Rozendal, R.; Schröder, U.; Keller, J.; Freguia, S.; Aelterman, P.; Verstraete, W.; Rabaey, K. (2006) Microbial Fuel Cells: Methodology and Technology†. *Environmental Science & Technology*, 40, 5181-5192.

Lu, N.; Zhou, S.-g.; Zhuang, L.; Zhang, J.-t.; Ni, J.-r. (2009) Electricity generation from starch processing wastewater using microbial fuel cell technology. *Biochemical Engineering Journal*, 43, 246-251.

Meehan, A.; Hongwei, G.; Lewandowski, Z. (2011) Energy Harvesting With Microbial Fuel Cell and Power Management System. *Power Electronics, IEEE Transactions on*, 26, 176-181.

Moqsud, M. A.; Omine, K.; Yasufuku, N.; Hyodo, M.; Nakata, Y. (2013) Microbial fuel cell (MFC) for bioelectricity generation from organic wastes. *Waste Management*, 33, 2465-2469.

Oh, S. E.; Logan, B. E. (2007) Voltage reversal during microbial fuel cell stack operation. *Journal of Power Sources*, 167, 11-17.

Rahimnejad, M.; Ghoreyshi, A. A.; Najafpour, G. D.; Younesi, H.; Shakeri, M. (2012) A novel microbial fuel cell stack for continuous production of clean energy. *International Journal of Hydrogen Energy*, 37, 5992-6000.

Sangeetha, T.; Muthukumar, M. (2013) Influence of electrode material and electrode distance on bioelectricity production from sago-processing wastewater using microbial fuel cell. *Environmental Progress & Sustainable Energy*, 32, 390-395.

Schroder, U. (2007) Anodic electron transfer mechanisms in microbial fuel cells and their energy efficiency. *Physical Chemistry Chemical Physics*, 9, 2619-2629.

Shantaram, A.; Beyenal, H.; Veluchamy, R. R. A.; Lewandowski, Z. (2005) Wireless Sensors Powered by Microbial Fuel Cells. *Environmental Science & Technology*, 39, 5037-5042.

Tang, H.; Cao, T.; Wang, A.; Liang, X.; Salley, S. O.; McAllister, J. P.; Ng, K. Y. S. (2007) Effect of surface modification of siliconeon Staphylococcus epidermidis adhesion and colonization. *Journal of Biomedical Materials Research Part A*, 80A, 885-894.

Tender, L. M.; Gray, S. A.; Groveman, E.; Lowy, D. A.; Kauffman, P.; Melhado, J.; Tyce, R. C.; Flynn, D.; Petrecca, R.; Dobarro, J. (2008) The first demonstration of a microbial fuel cell as a viable power supply: Powering a meteorological buoy. *Journal of Power Sources*, 179, 571-575.

Thomas, Y. R. J.; Picot, M.; Carer, A.; Berder, O.; Sentieys, O.; Barrière, F. (2013) A single sediment-microbial fuel cell powering a wireless telecommunication system. *Journal of Power Sources*, 241, 703-708.

Wang, H.; Park, J.-D.; Ren, Z. J. (2015) Practical Energy Harvesting for Microbial Fuel Cells: A Review. *Environmental Science & Technology*, 49, 3267-3277.

Winfield, J.; Chambers, L. D.; Stinchcombe, A.; Rossiter, J.; Ieropoulos, I. (2014) The power of glove: Soft microbial fuel cell for low-power electronics. *Journal of Power Sources*, 249, 327-332.

Yang, S.; Jia, B.; Liu, H. (2009) Effects of the Pt loading side and cathode-biofilm on the performance of a membrane-less and single-chamber microbial fuel cell. *Bioresource Technology*, 100, 1197-1202.

Yang, X.; Beyenal, H.; Harkin, G.; Lewandowski, Z. (2000) Quantifying biofilm structure using image analysis. *Journal of Microbiological Methods*, 39, 109-119.

Zhang, D.; Yang, F.; Shimotori, T.; Wang, K.-C.; Huang, Y. (2012) Performance evaluation of power management systems in microbial fuel cell-based energy harvesting applications for driving small electronic devices. *Journal of Power Sources*, 217, 65-71.

Zhang, F.; Tian, L.; He, Z. (2011) Powering a wireless temperature sensor using sediment microbial fuel cells with vertical arrangement of electrodes. *Journal of Power Sources*, 196, 9568-9573.

Zhang, J.; Li, J.; Ye, D.; Zhu, X.; Liao, Q.; Zhang, B. (2014) Tubular bamboo charcoal for anode in microbial fuel cells. *Journal of Power Sources*, 272, 277-282.

Zhang, Y.; Angelidaki, I. (2012) Self-stacked submersible microbial fuel cell (SSMFC) for improved remote power generation from lake sediments. *Biosensors and Bioelectronics*, 35, 265-270.

Zhuang, L.; Zheng, Y.; Zhou, S.; Yuan, Y.; Yuan, H.; Chen, Y. (2012) Scalable microbial fuel cell (MFC) stack for continuous real wastewater treatment. *Bioresource Technology*, 106, 82-88.

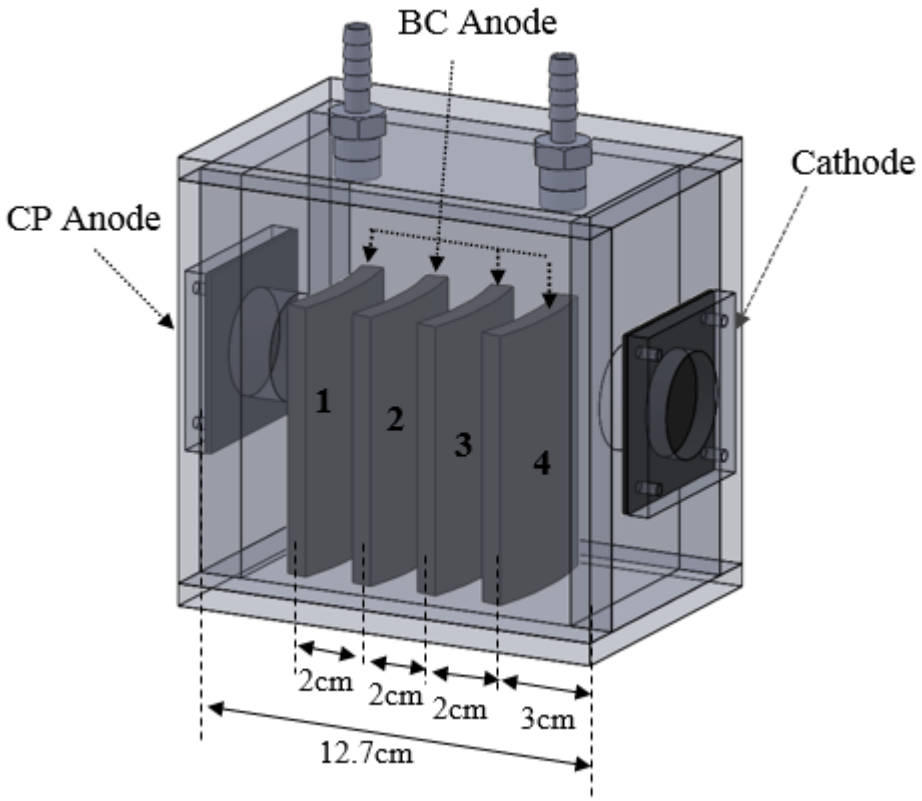

Figure 3-1: Air-cathode SCMFC with a carbon paper (CP) anode and four bamboo-charcoal (BC) anode plates.

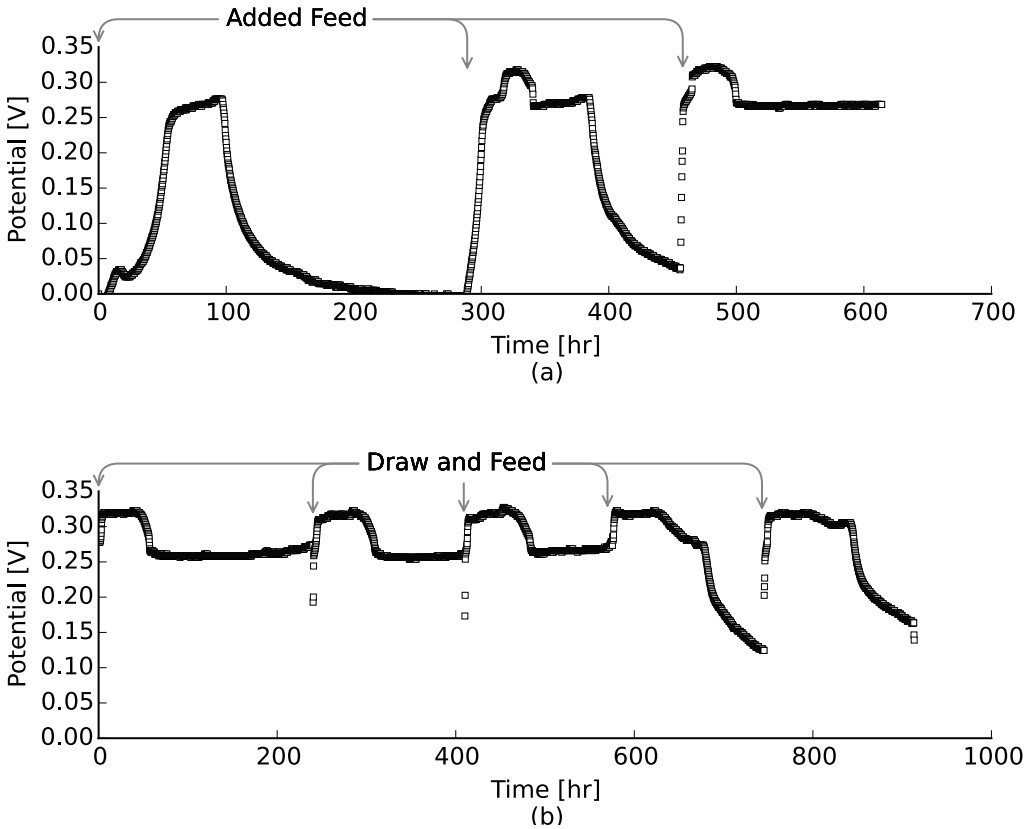

Figure 3-2: (a) Voltage output measured at external resistance of 1kΩ during the incubation period. (b) Voltage output measured at external resistance of 1kΩ during cycle 4 through cycle 8. (Note: the 0 hours correspond to 614 hours, i.e., where (a) left off)

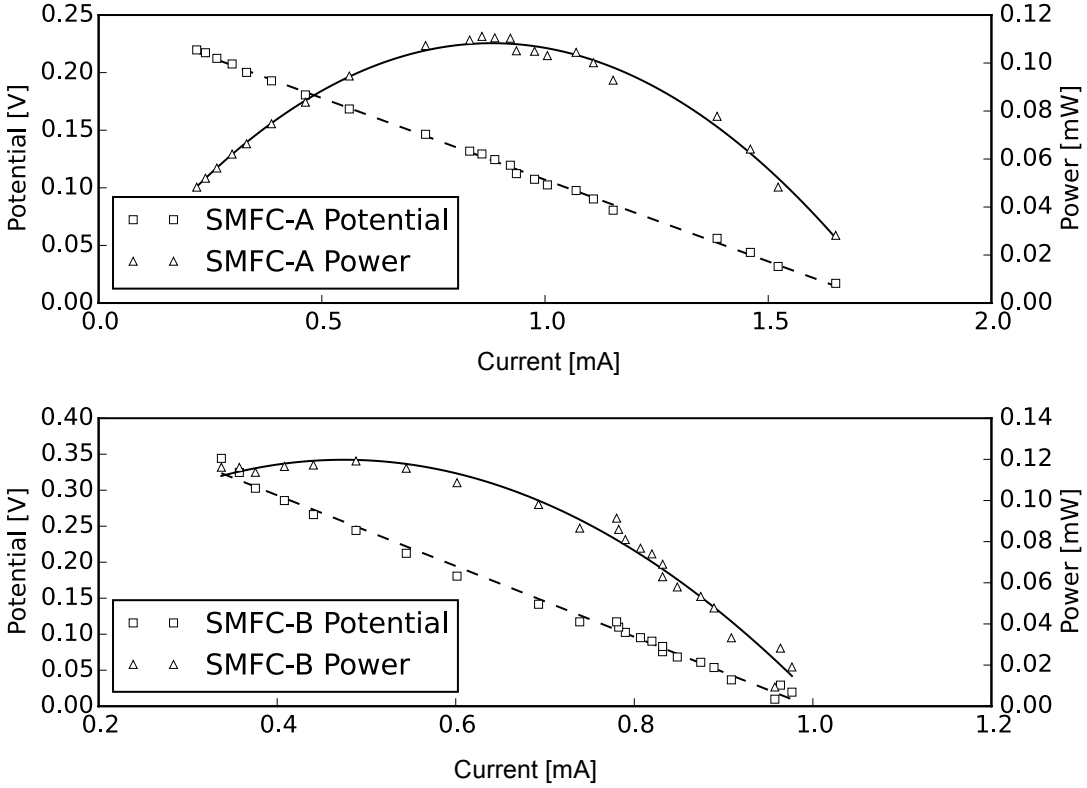

Figure 3-3: Polarization curves and power-current curve for the highest potential producing anodes in (a) SMFC-A and (b) SMFC-B.

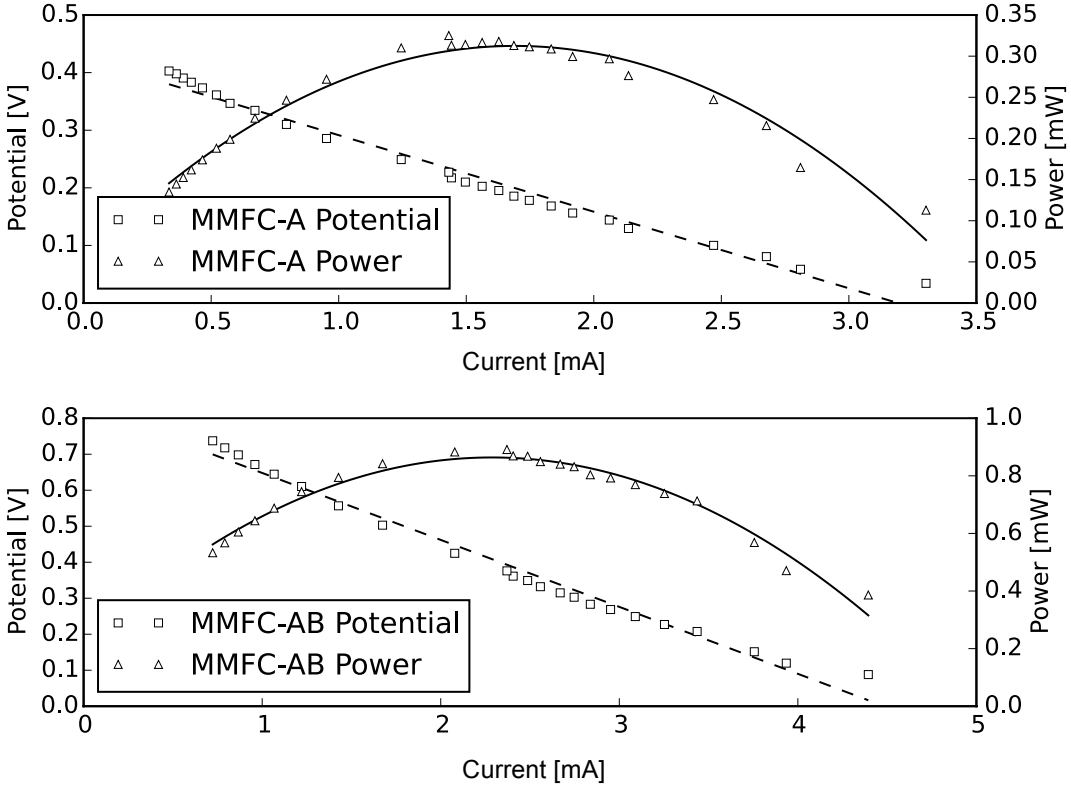

Figure 3-4: (a) Polarization curves and power-current curves for MFC-A with all anodes connected (MMFC-A); (b) MMFC-A and MMFC-B in series with all anodes connected (MMFC-AB).

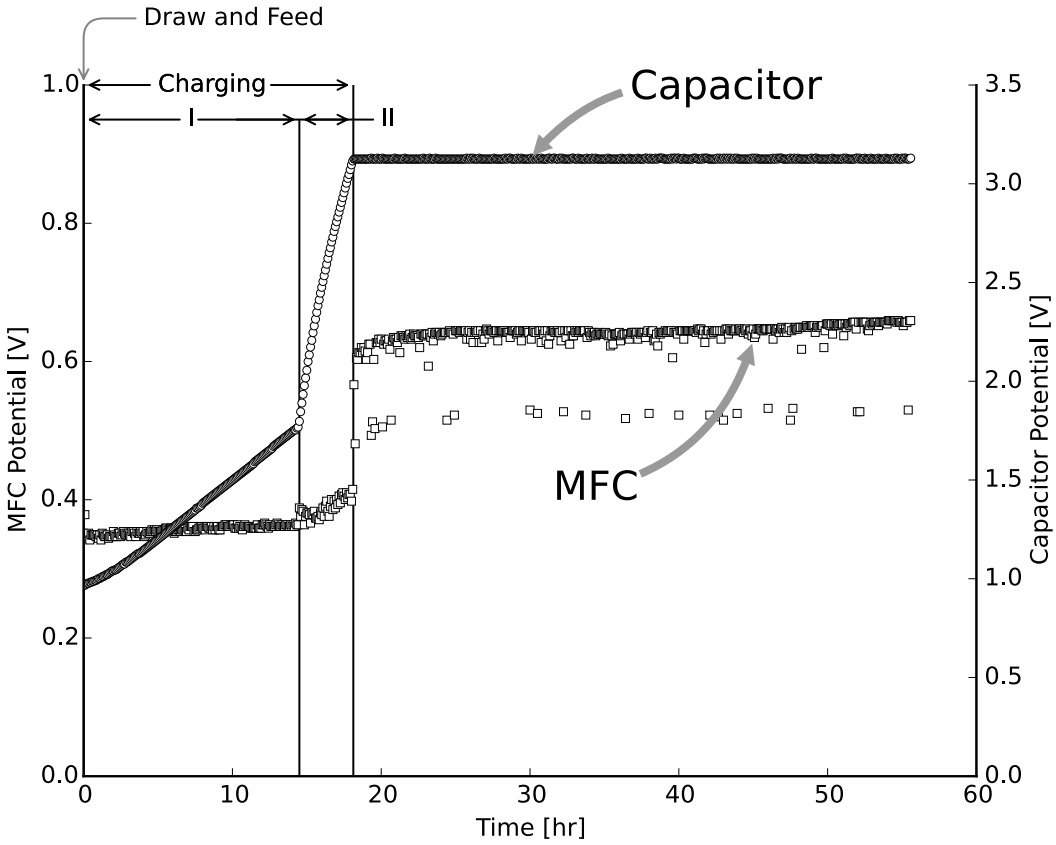

Figure 3-5: Charging the capacitor with SMFC-A and SMFC-B in series using the Energy Harvester.

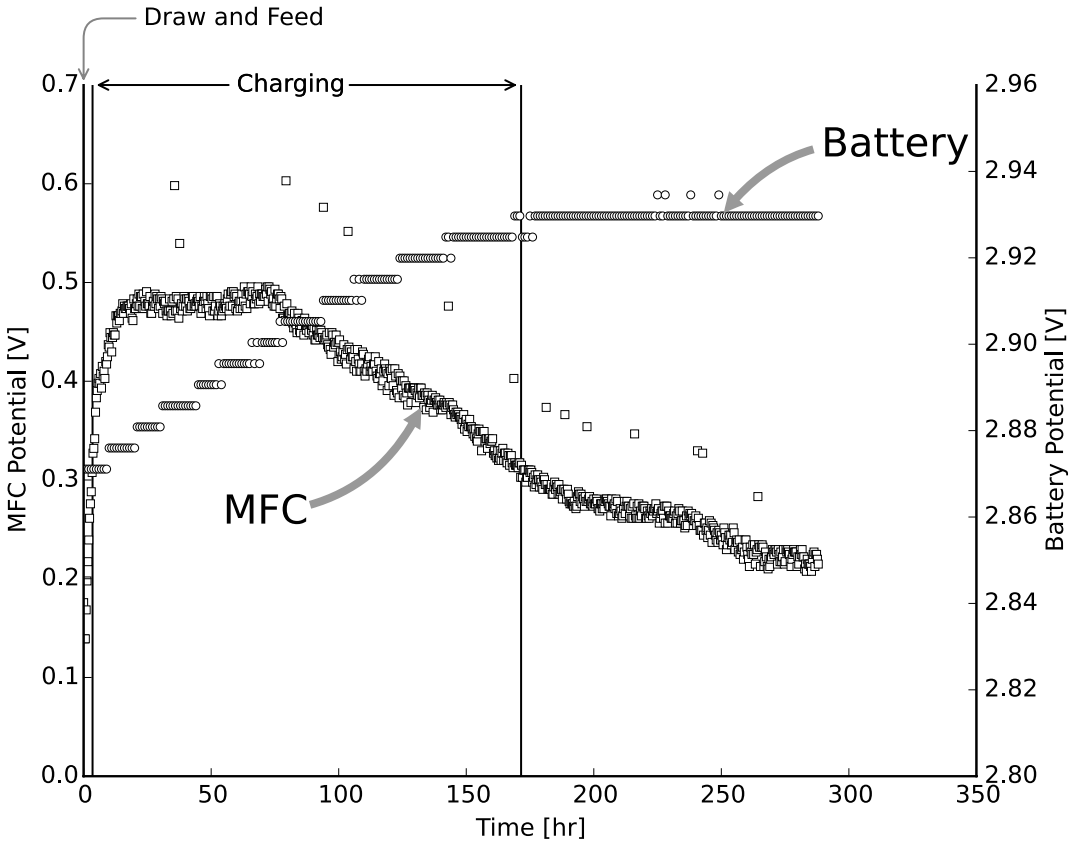

Figure 3-6: Charging the battery with SMFC-A and SMFC-B in series using the Energy Harvester.

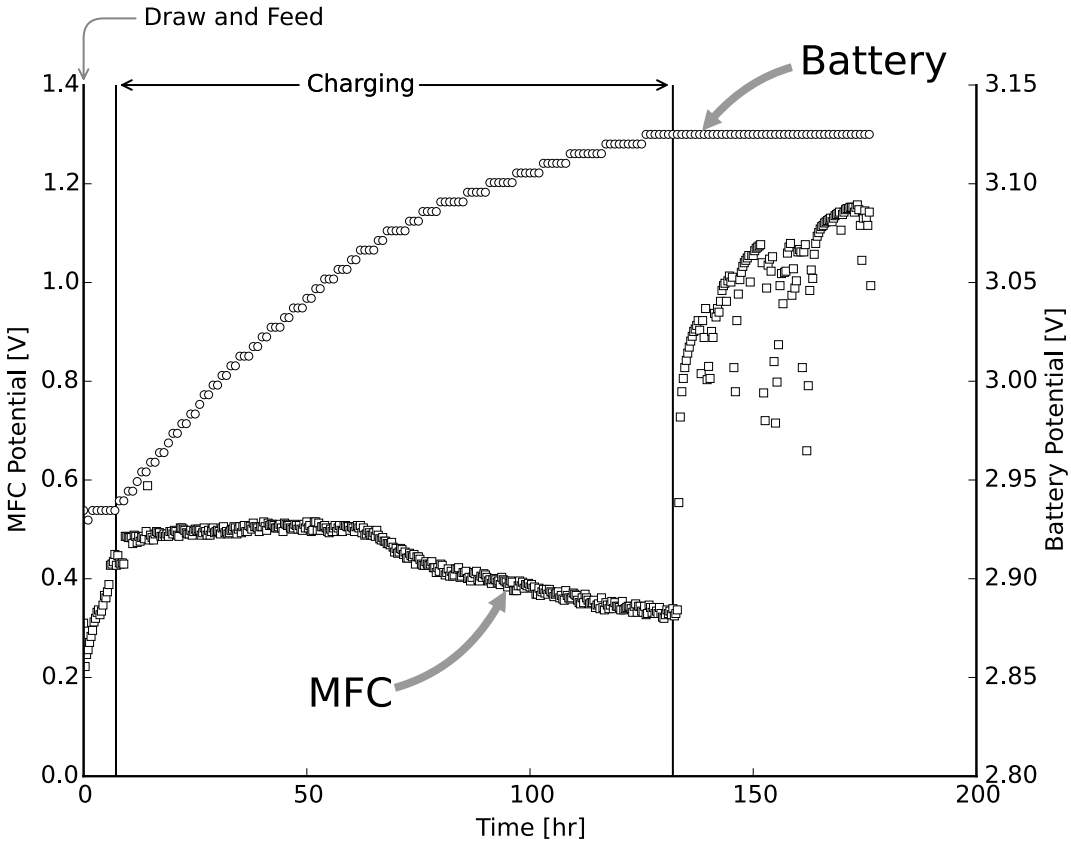

Figure 3-7: Charging the battery with MMFC-A and MMFC-B in series using the Energy Harvester.

Table 3-1: Summary of power generation among different configurations

Configuration		Potential [V]	Current [mA]	Power [mW]	Cathode Area		Substrate Volume		Anode Area	
					Power Density [mW/m^2]	Current Density [mA/m^2]	Power Density [mW/m^3]	Current Density [mA/m^3]	Power Density [mW/m^2]	Current Density [mA/m^2]
Single Anode	SMFC-A	0.12	0.88	0.11	164	1315	220	1762	12.9	103
	SMFC-B	0.25	0.48	0.12	179	716	240	960	14.1	56.3
Multiple Anode	MMFC-A	0.23	1.41	0.32	478	2106	640	2819	9.39	41.4
	MMFC-AB	0.38	2.37	0.89	1328	3533	1780	4734	13.1	34.8

CHAPTER 4

Summary

In this study, a novel single chamber microbial fuel cell having multiple anode plates of bamboo charcoal (MAP-SCMFC) was developed. A significant advantage of this design is that it allows simultaneous voltage measurements at individual anode plates located at different distances from the cathode. In the first phase of this study, the effects of the electrode spacing on the power output and internal resistance were evaluated using the MAP-SCMFC-A. In the second phase, an additional MAP-SCMFC-B was constructed and connected to the MAP-SCMFC-A in series. This configuration of the MAP-SCMFCs boosted the power output, sufficient to charge a capacitor and battery.

In the study with MAP-SCMFC-A, the peak potential was the smallest amongst all the anodes at the carbon paper (CP) anode located at the furthest distance from the cathode. Among the bamboo charcoal (BC) anodes, voltage reached the highest peak but declined most rapidly with the bamboo charcoal anode located closest to the cathode (BC4). On the other hand, voltage reached the lowest peak but decreased at the slowest rate with the bamboo charcoal located farthest from the cathode (BC1). The order of the peak voltages measured with the individual anodes (identified by the distance measured from the cathode) are 0.288 V at the CP anode (12.7 cm), 0.303 V at the BC1 anode (9 cm) and BC2 anode (7 cm), 0.308 V at the BC3 anode (5 cm), and 0.313 V at the BC4 anode (3 cm). The largest maximum power density (168 mW/cm^2) and smallest internal resistance (141 Ω) were produced by the BC4 anode, whereas the smallest maximum power density (125 mW/cm^2) and largest internal resistance (158 Ω) were yielded by the BC1 anode. The increase of the internal resistance with the increase of the distance

between the cathode and the anode was estimated to be 2.83 Ω/cm. When all the anodes were connected together (CP-BC1-BC2-BC3-BC4), the MAP-SCMFC produced the largest power density of 504 mW/cm^2 with an internal resistance of 118 Ω.

When two MAP-SCMFCs (MAP-SCMFC-A and MAP-SCMFC-B) were connected in series and all the anodes were connected together (denoted by MMFC-AB), the system produced the largest power density of 1,328 mW/m^2 of cathode area and 13 mW/m^2 of anode area. When MAP-SCMFC-A and MAP-SCMFC-B, with single BC anode plate, were connected in series (SMFC-AB), it generated sufficient power to charge a capacitor and a battery. The MMFC-AB reduced the charging time by a factor of 4.3 as compared to the SMFC-AB. The charged battery yielded the capacity rating of 13mAh (Energy=38 mWh), indicating that the MAP-SCMFC system has potential to be used in running a low power device.

For future studies, bamboo charcoal can be prepared in lab by selecting good quality bamboo wood to ensure low internal resistance of the bamboo charcoal. The MFCs can be scaled up to a greater volume than what has been used in this study, and more than two reactors can be connected in series for higher power production. Inside each reactor, the number of bamboo charcoal plates can be increased, and experiments can be run using several possible orientations for placing these charcoal plates inside the chamber.

APPENDIX

Appendix A Preliminary Study of Bamboo Charcoal as an Anode MFC and Test Setup

The preliminary study implemented a single chamber microbial fuel cell (SCMFC) that was used in the previous thesis experiment (Sharma, 2008). The SCMFC used bamboo charcoal (Mt Meru Pte Ltd, Singapore). It was cut in half to allow it to fit in the anode chamber. No other preparation to the bamboo charcoal was performed. A small hole was drilled into the charcoal to allow the platinum wire to be inserted. The hole was then filled with J-B Weld (J-B Weld, Sulphur Springs,TX).

The SCMFC was operated in a draw-and-feed process, which consists of removal of used substrate solution (spent fuel), and refilling with a fresh feed solution. This operation was conducted in a glove chamber filled with pressurized nitrogen (N_2) gas. The experiment was carried out with two different concentrations of feed solutions: 0.25% (~ 300 mg/L BOD_5) and 0.50% (~ 600 mg/L BOD_5). The potential was recorded at 15-minute intervals using a data acquisition system with an external resistance of 990 Ω, the results are discussed in the following section.

Results

Figure A-1 shows electrical potential produced by the SCMFC at feed concentrations of 0.25% and 0.5%. The peak potential for 0.50% is 60% greater than that for 0.25%. The runs end after about 250 hours, which is much greater than observed in previous SCMFC testing in Sharma (2008). However, longer run times are expected since the volume of the reactor is larger than that used in Sharma (2008). One interesting observation is that doubling the feed concentration did not affect the runtime of the reactor. The test reactors in Sharma (2008) showed an increase in runtime when the concentration was increased. This may imply that bamboo charcoal anode can handle

even higher concentration than the SCMFC used in Sharma (2008). A previously used cathode was reused in the reactor, which may have resulted in lower performance. Using a new cathode can possibly improve the performance.

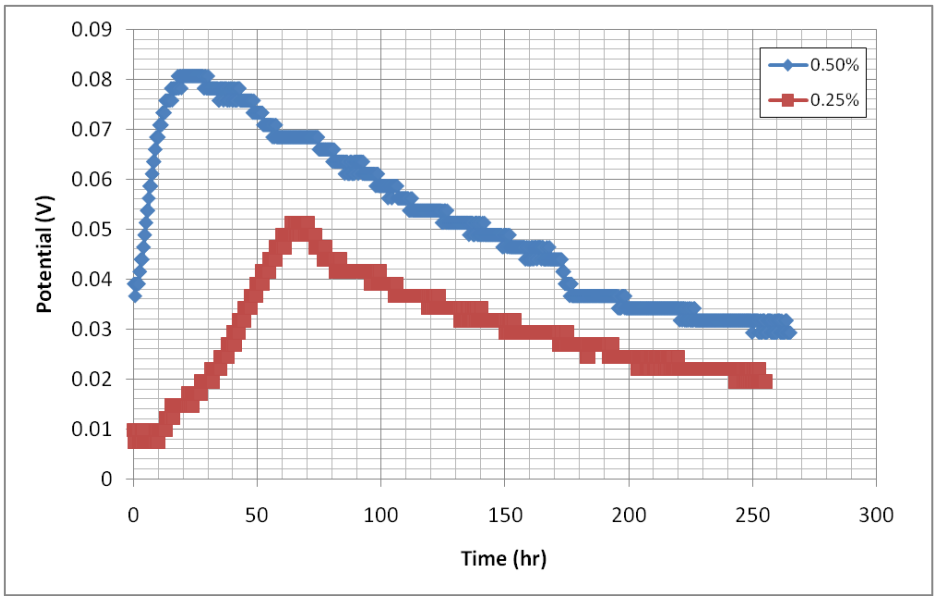

Figure A-1: Results from preliminary study

Reference

Sharma, R. (2008) Effect of surface areas of electrodes on the performance of a single-chamber microbial fuel cell, Civil and Environmental Engineering. Idaho State University.

Appendix B MFC metabolism

The biodegradation of organic matter takes place in the anodic chamber where microorganisms catabolize compounds such as domestic wastewater to generate electrons and protons. Unlike in a direct combustion process, the electrons released from oxidation of these organic substances are transferred to the anode, then flow through the electrical circuit to the cathode. In a dual chamber microbial fuel cell (DCMFC), the protons (H^+) travel via the substrate to the cathodic chamber where they combine with oxygen to form water. The anode chamber is maintained anaerobic so that the only means of respiration for these microorganisms is to transfer electrons to the anode, therefore generating electric current. As current flows over a potential difference, power is generated directly from biofuel by the catalytic activity of bacteria (Rabaey and Verstraete, 2005). Carbon dioxide is produced as an oxidation product. In a DCMFC, CO_2 is collected in the anode chamber headspace and H_2 in the cathode headspace. In a single-chamber configuration, both gases are collected in the same headspace (Gabriel, 2010). However, there is no net carbon emission because the carbon dioxide in the renewable biomass originally comes from the atmosphere in the photosynthesis process (Du et al., 2007). The other major components of the organic compounds, nitrogen and phosphorus exist as NH_4^+ and orthophosphate (PO_4^{3-}, HPO_4^{2-}, $H_2PO_4^-$, H_3PO_4), respectively. Small fractions are consumed by the microorganisms, help towards the bacterial growth, and partly accumulate on the electrode surfaces as biomass in an MFC.

The bacterial metabolism in the process of electricity generation by a two-chambered MFC and a single-chambered MFC are shown in Figures B-1 and B-2, respectively.

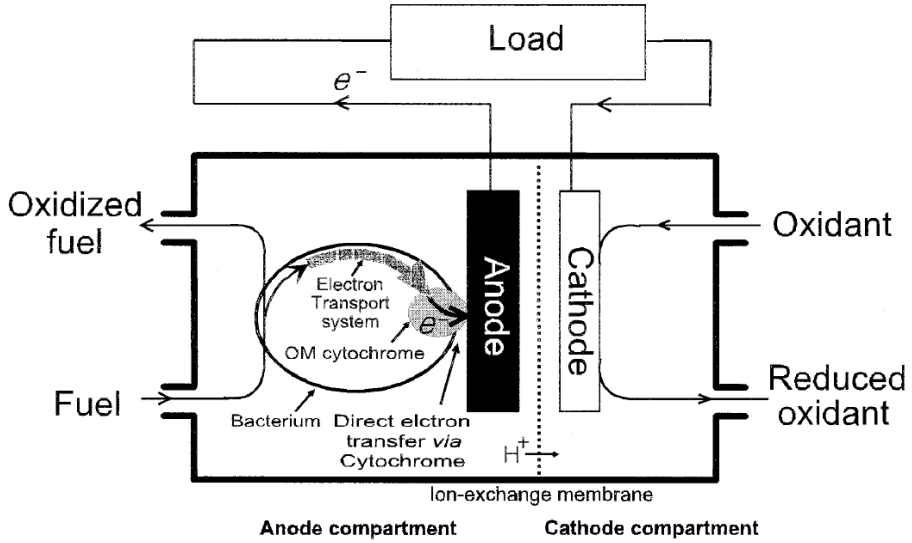

Figure B-1: Schematic diagram showing bacterial activity in the anode chamber in a two-chamber microbial fuel cell (Kim et al., 2007)

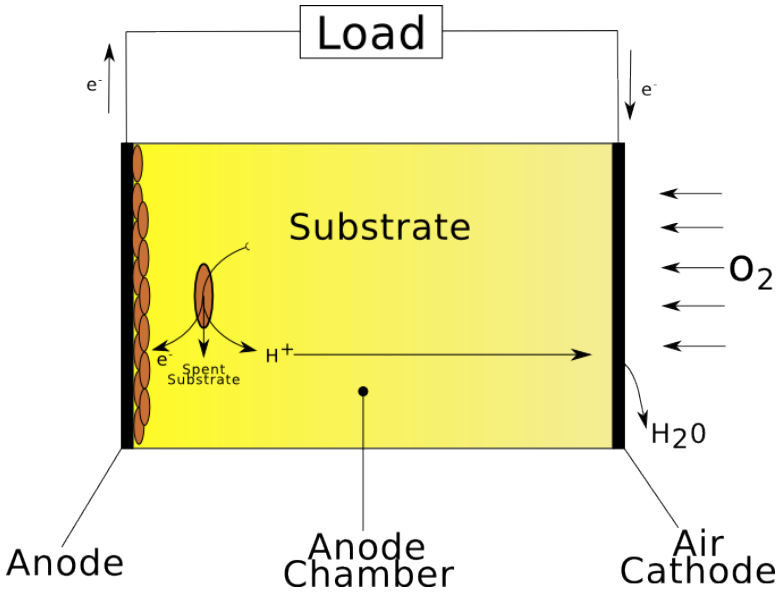

Figure B-2: Schematic diagram showing bacterial activity in a single chamber microbial fuel cell

The electrochemical potential between the respiratory enzyme and the electron acceptor at the cathode follows a voltage output profile as shown in Figure B-3.

The voltage curve has three stages. The first stage is where there is more available food; therefore there is an increase in bacteria population resulting in high potential increase. The second stage represents the phase of maximum substrate utilization producing maximum potential with constant output. The third stage is where there is limited food supply; therefore there is a decrease in bacteria number, resulting in the decrease in potential.

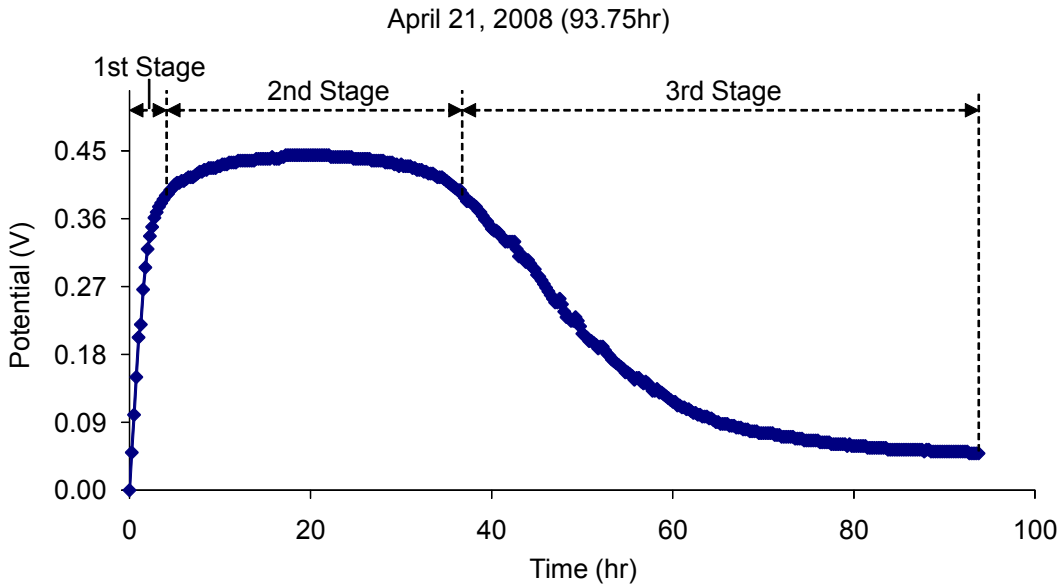

Figure B-3: A typical voltage output profile shown by SCMFC fed with 300 mg/L BOD_5 (0.25% v/v) potato wastewater

References

Bitton, G. (2010) *Wastewater Microbiology*. 4 ed. Wiley.

Du, Z.; Li, H.; Gu, T. (2007) A state of the art review on microbial fuel cells: A promising technology for wastewater treatment and bioenergy. *Biotechnology Advances*, 25, 464-482.

Kim, J. R.; Cheng, S.; Oh, S.-E.; Logan, B. E. (2007) Power Generation Using Different Cation, Anion, and Ultrafiltration Membranes in Microbial Fuel Cells. *Environmental Science & Technology*, 41, 1004-1009.

Rabaey, K.; Verstraete, W. (2005) Microbial fuel cells: novel biotechnology for energy generation. *Trends Biotechnol*, 23, 291-298.

Appendix C Fully Constructed MAP-SCMFC

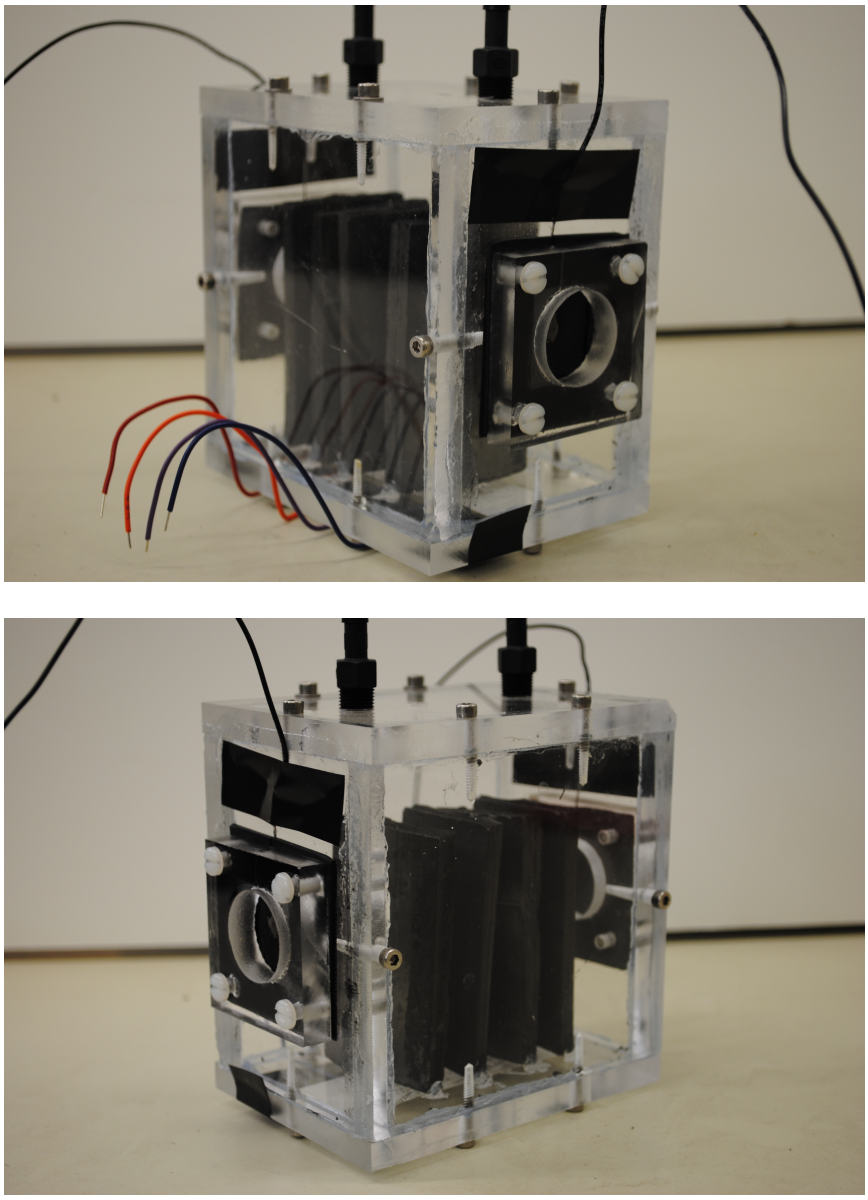

Figure C-1: Fully constructed MAP-SCMFC-A

Appendix D Data Acquisition and Connections

Equipment and materials

- National Instrument (NI) connection block, SCB-68.
- Insulated 32 AWG (American Wire Gauge) wire, 2 pieces, 3 meters long.
- Nominal Resistors, 1000 kΩ
- Alligator clips, 2 pieces, 2 cm size.
- Liquid silver solder, CircuitWriter™ Conductive Pen, electric resistance (<0.020 Ω/sg/mil) from CAIG Laboratories, Inc. 12200 Thatcher Court, Poway, CA, 92064.
- Tools including pliers or wire crimpers, and screw drivers.

MFC with anode individually connected

- A wire from each anode was connected to a separate channel on the DAS Board

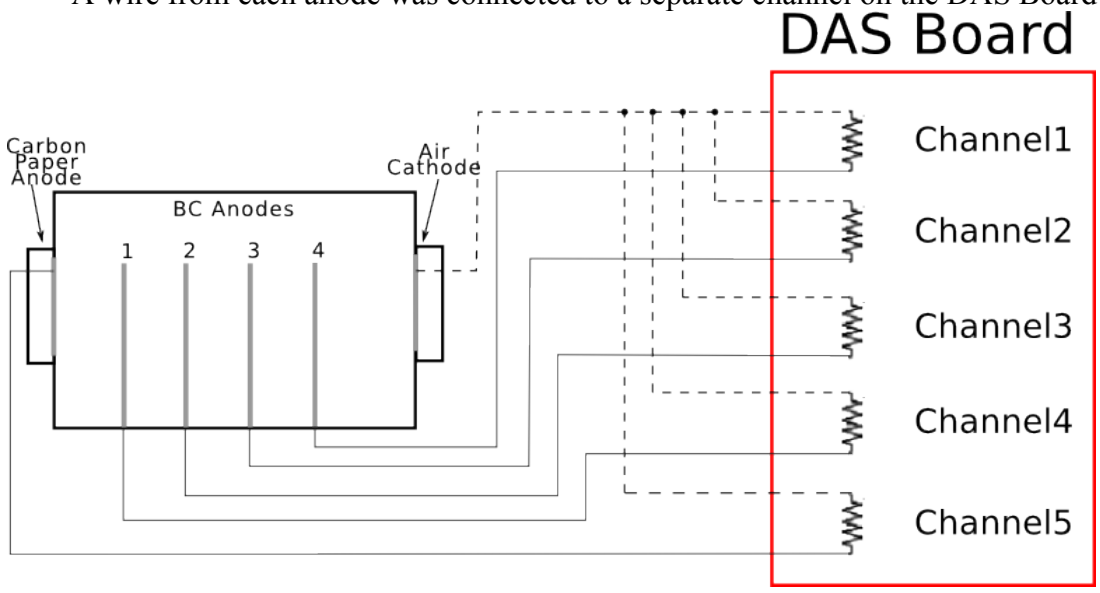

Figure D-1: Connection scheme for MFC with anodes individually connected.

MFC with all anode connected together

- Each wire from the anodes were connected to the same channel on the DAS Board

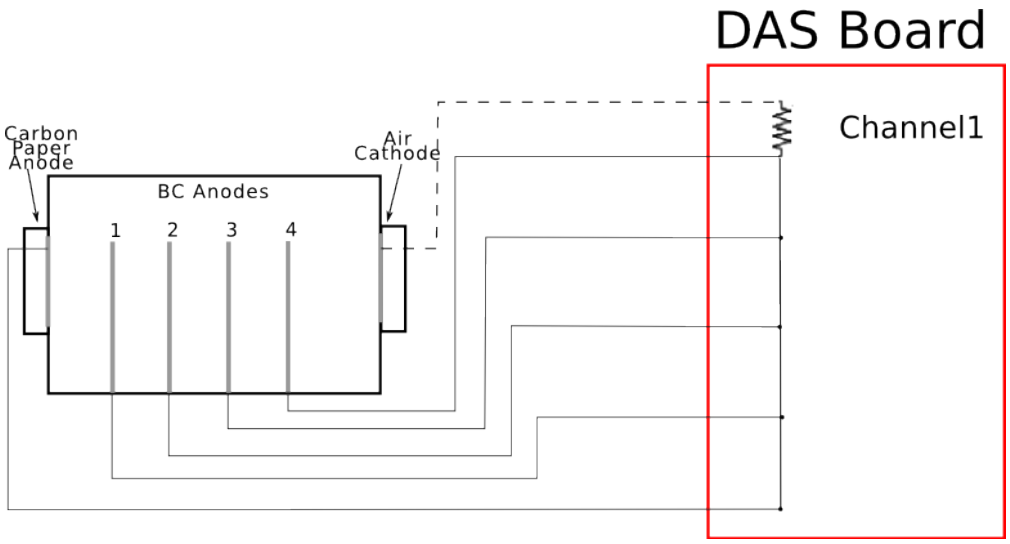

Figure D-2: Connection scheme for MFC with all anodes connected together.

Energy harvester circuit connection with capacitor – Minimum configuration

- The anode from each MFC was connected to a separate channel on the DAS board
- The voltage input to Energy Harvester was connected to separate channel on the DAS board, i.e., the MFC in series.
- The voltage of the capacitor as it was being charged by the energy harvester was connected to a separate channel on the DAS board

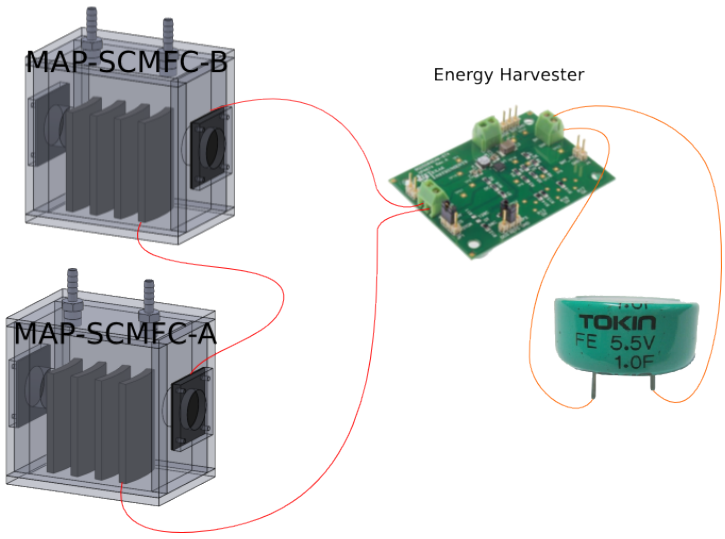

Figure D-3: Connection scheme for MFCs in series with an Energy Harvester charging a Capacitor

Energy harvester circuit connection with battery – Minimum configuration

- The anode from each MFC was connected to a separate channel on the DAS board
- The voltage input to Energy Harvester was connected to separate channel on the DAS board, i.e., the MFC in series.
- The voltage of the battery as it was being charged by the energy harvester was connected to a separate channel on the DAS board

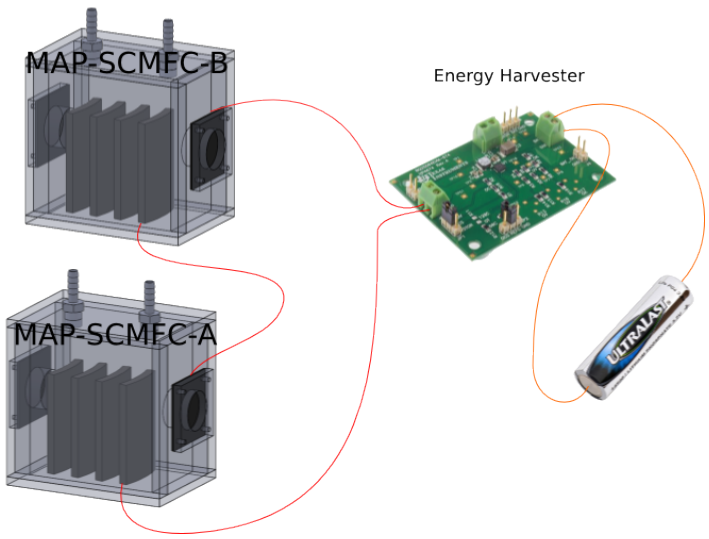

Figure D-4: Connection scheme for MFCs in series with an Energy Harvester charging a Battery

Energy harvester circuit connection with battery – Maximum configuration

- The anodes from each MFC were connected to a one channel on the DAS board, same connection as described in the MFC with all Anodes Connected Together Section
- The voltage input to Energy Harvester was connected to separate channel on the DAS board, i.e., the MFC in series.
- The voltage of the battery as it was being charged by the energy harvester was connected to a separate channel on the DAS board

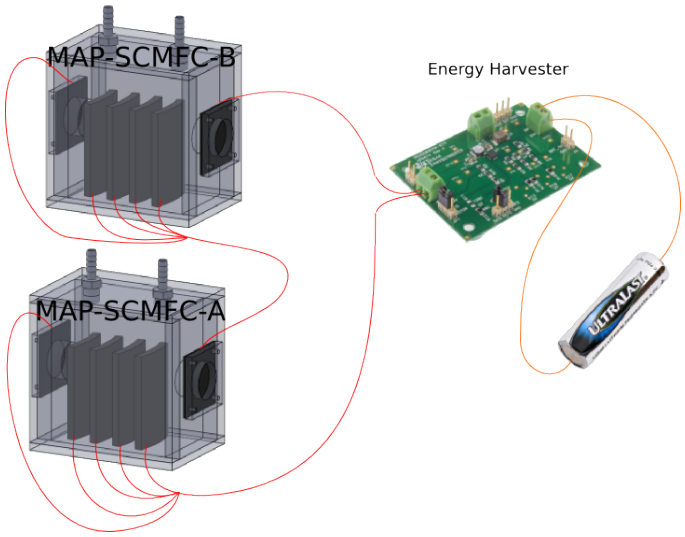

Figure D-5: Connection scheme for MFCs in series with an Energy Harvester charging a Capacitor

Appendix E Additional Results from MAP-SCMFC-A

MAP-SCMFC-A demonstrated reproducible patterns from sixth cycle and onward. This indicated that the MFC was fully established.

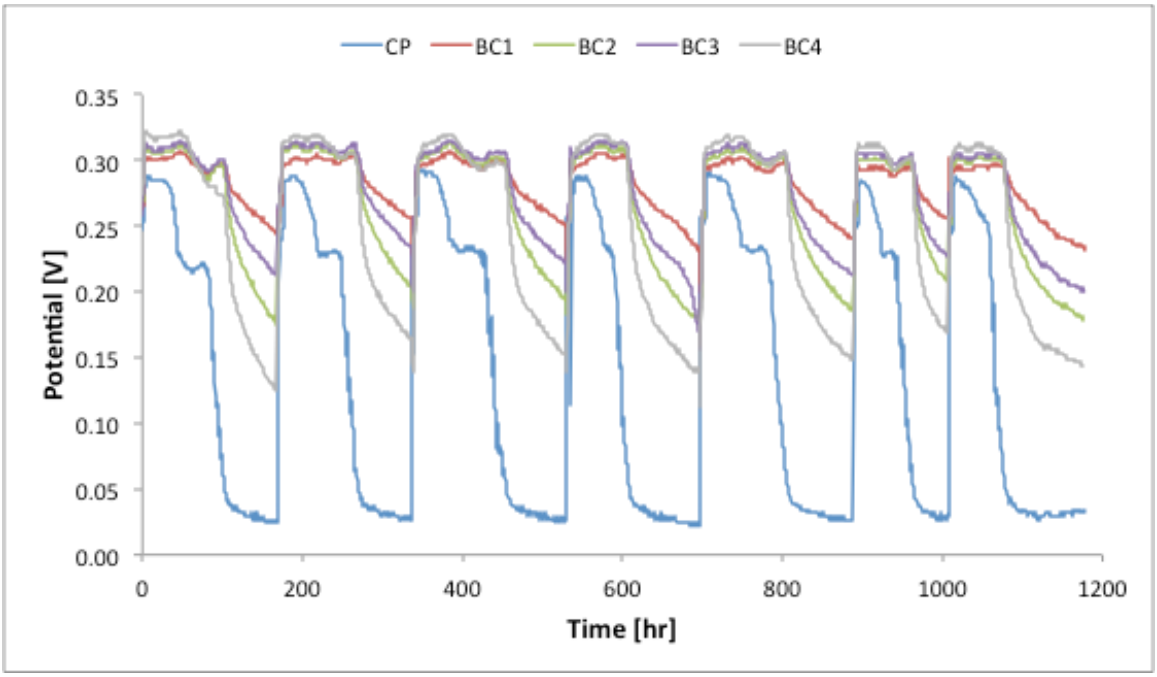

Figure E-1: MAP-SCMFC-A reproducible cycles.

Comparison of Polarization curves for MAP-SCMFC-A with all anodes connected versus the anode closet to the cathode are shown in Figure E-2 with the following differences:

- Internal resistance decreased: 118Ω
- Power density increased: 504 mW/m^2
- Current density increased: 2520 mA/m^2

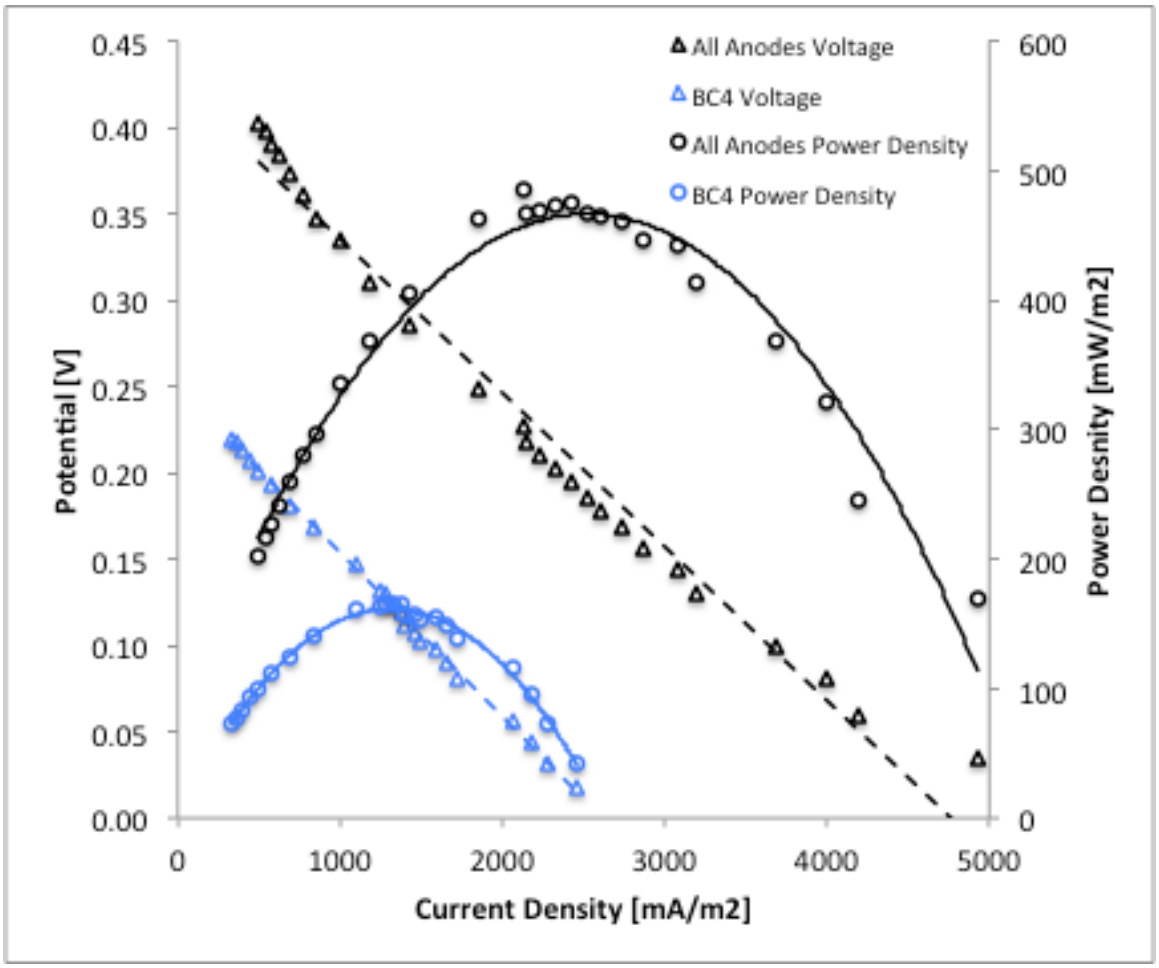

Figure E-2: Comparison of Polarization curves for MAP-SCMFC-A with all anodes connected versus the anode closet to the cathode.

Appendix F Preparation of feed solution

Sterilization of wastewater

Equipment and materials:

- Autoclave, Model 2540E, Tuttnauer Co. Ltd., Jerusalem, Israel.
- Refrigerator, Diplomat, Danby Refrigerator, Findlay, OH, 45839.
- Wastewater from the primary clarifier, Pocatello Wastewater Treatment Plant.
- Glassware
- Gloves

Procedures:

- Take the Pyrex bottles with the samples from the refrigerator and loosen the lids.
- Place the bottles inside the autoclave.
- Set the autoclave at disinfection cycle (60 minutes at 121ºC), lock the door by turning the handle clockwise.
- After the disinfection cycle is done, and the system is cool, open the door and securely tighten the lids.
- Place the bottles in the refrigerator (~4ºC).

Preparation of Buffer

Equipment and materials:

- Sodium Phosphate Monobasic ($NaPO_4 \cdot H_2O$)
- Sodium Phosphate Dibasic Anhydrous (Na_2PO_4H)
- 1M Sodium Hydroxide (NaOH)
- 1M Hydrochloric acid (HCl)
- De-ionized (DI) water

- Analytical balance, XE Series Model 100A, Denver Instrument Company, Arvada, CO, 80004.
- Auto mixer and hot plate, Fisher Scientific, USA.
- pH meter. Model 250A, Orion Research Inc, Boston, MA.
- 1000 mL Flask
- Pyrex bottle, 1000 mL capacity.
- Gloves

Procedures:

- Weigh 53.8 g of monobasic $NaPO_4 \cdot H_2O$
- Weigh 86.59 g of dibasic Na_2PO_4H
- Pour both components into an Erlenmeyer flask (1000 mL capacity).
- Fill the flask up to the 1000 mL level with DI water.
- Turn on the stir setting to a speed of 7 and turn on the heat setting to 2. Stir and heat until the solution is clear and the components are complete dissolved.
- Verify the pH of solution is neutral (pH=7) with a pH meter. If solution is acidic (pH<7) add NaOH until solution is neutral. If solution is alkaline (pH>7) then add HCl until the solution is neutral.

Preparation of Feed Solution

Equipment and materials:

- Buffer (pH=7)
- De-Ionized (DI) water
- Basic American Food (BAF) Potato Concentrate
- Pipetaid, Drummond Scientific Co. Broomall, PA, 19008.

- 250 mL glass bottles with caps
- Autoclave, Model 2540E, Tuttnauer Co. Ltd, Jerusalem, Israel.
- Parafilm, Laboratory Film, Pechiney Plastic Packaging, Chicago, IL, 60631.
- Refrigerator, Diplomat, Danby Refrigerator, Findlay, OH, 45839.
- Glassware

Procedures:

- In a 1000 mL cylindrical beaker, add 2.5 mL of BAF.
- In a separate 1000 mL cylindrical beaker, add 100 mL of Buffer. Then add and mix 1000 mL of DI water, making a 0.1M solution.
- Add the 0.1M solution to the cylindrical beaker containing the BAF filling to the 1000 mL line.
- Divide the solution into four glass bottles (250 mL capacity), put the caps on loosely.
- Autoclave the bottles in the disinfection cycle (60 minutes at 121ºC).
- After autoclaving the samples and cool down, securely tighten the caps and seal with parafilm.
- Store in the refrigerator.

Appendix G Biological Oxygen Demand (BOD_5) Procedures

Equipment and materials:

- BOD Nutrient Buffer Pillows, HACH Company, P.O. BOX 389, Loveland, CO, 80539.
- Polyseed® BOD seed inoculums, Lot 3199032, 12405 Sowden Road, Houston, TX, 77080.
- DO meter set, Oxi 315i/SET, Dissolve Oxygen Meter, WTW Wissenschaftlich-Technische Werkstätten, 82362, Weilheim, Germany.
- Analytical balance, XE Series Model 100A, Denver Instrument Company, Arvada, CO, 80004.
- Incubator REVCO Model BOD50, Asheville, NC.
- BOD bottles, 300 mL capacity.
- BOD plastic caps
- De-ionized (DI) water
- Auto mixer, Fisher Scientific, USA.
- Fish tank aerator
- Pipette
- Glassware
- Gloves

Figure G-1: BOD nutrient pillows and Polyseed® for the BOD_5 test

Procedures:

- Preparation of dilution water (Prepare the solution ~24 hours prior to the experiment).
    - Pour 9 L of de-ionized (DI) water in a container and add the content of 3 BOD Nutrient Buffer Pillows.
    - Shake well to mix.
    - Put the fish tank aerator into the container to aerate the water.

Figure G-2: Aeration of dilution water

- Preparation of seed solution.
    - Pour 500 mL of de-ionized (DI) water in a beaker and add the content of one capsule of Polyseed® to the water.
    - Stir for approximately one hour in the auto mixer.

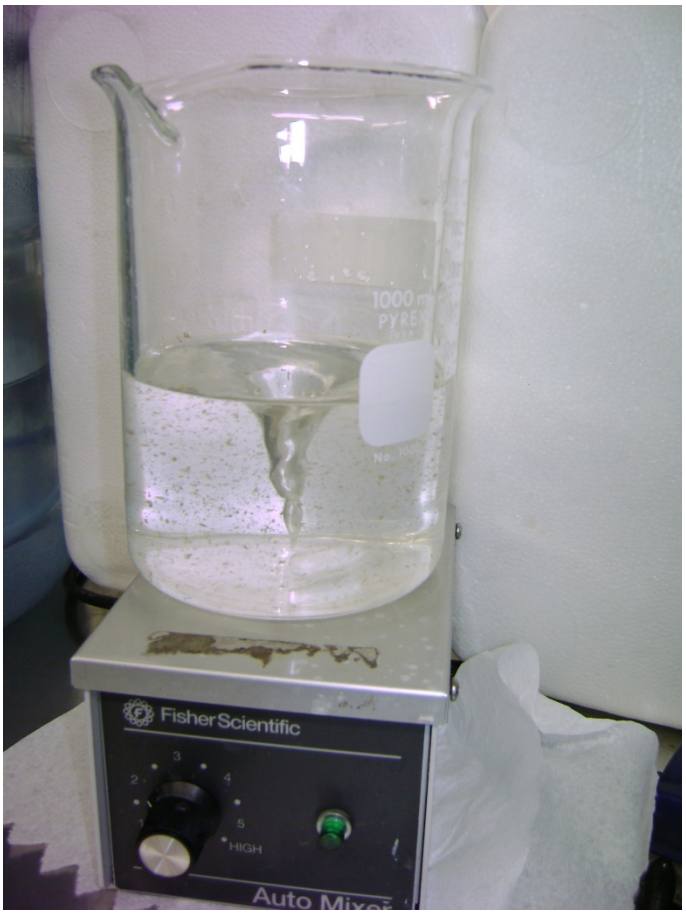

Figure G-3: Preparation of seed solution

- Preparation of BOD bottle samples.

To each bottle:

  - Add 0.5 mL of seed solution.
  - Add the appropriate quantity of sample to be tested (sample size ranges from 1 mL- 20 mL).
  - Fill the BOD bottle about 1 inch from the top of the bottle with dilution water.
  - Put in the glass stopper.
  - Invert the bottle several times to mix.

- Add enough dilution water to the lid of the BOD bottle to make a water seal, and put on the plastic caps (for the 5-day bottles).
- Put the 5-day BOD bottles in an incubator at 20±1ºC, to incubate in the dark for five days.

Figure G-4: Preparation of BOD bottles

- Measurement of dissolve oxygen (DO) of sample.
  - Remove wetting cap from the sensor.
  - Switch meter "ON".
  - Place the sensor inside the BOD bottle.
  - Press "AR" and then "RUN/ENTER".
  - The "AR" in the display will blink while making the reading.
  - The reading is done when the "AR" sign is steady.

- Repeat the process for initial day measurement and the 5-day measurement.

- Calculation of the BOD_5.
  - $DilutionFactor = \frac{SampleVolume(mL)}{BODbottleCap(mL)}$
  - $*F = (B_1 - B_5)avg * (Rs_1 \div Rs_2)$
    - B_1 = DO reading for blank sample in day 1
    - B_5 = DO reading for blank sample in day 5
    - Rs_1 =seed solution (mL) add to blank
    - Rs_2 = seed solution (mL) add to samples
  - $BOD_5 = \frac{\left[(D_1 - D_5) - *F\right]}{DilutionFactor}$
    - D_1 = DO reading for sample in day 1
    - D_5 = DO reading for sample in day 5

Appendix H Biological Oxygen Demand (BOD_5) Results

Table H-1: BOD5 Calculations

Solution Type	Bottle #	Seed (mL)	Sample (mL)	mL Dilution water fill to	Dilution factor (fracton)				F	BOD5
	(1)	(2)	(3)	(4)	(5)	(6)	(7)	(8) (6)-(7)	(9) *	(10) (8)/(5)
		Rs2				B1	B2	B1-B2		
SEED	1	0.5		300		5.7	5.6	0.1		
	2	0.5		300		5.7	5.5	0.2		
							Avg	0.15		
		Rs1				D1	D2	D1-D2		
IN	1	0.5	0.3	300	0.001	5.7	5.0	~~0.7~~	0.15	~~660.0~~
0.25%	2	0.5	0.5	300	0.002	5.7	4.5	~~1.2~~	0.15	~~630.0~~
	3	0.5	0.8	300	0.003	5.7	3.9	~~1.8~~	0.15	~~660.0~~
	4	0.5	1.0	300	0.003	5.7	3.2	2.5	0.15	705.0
	5	0.5	1.5	300	0.005	5.7	2.2	3.5	0.15	670.0
									Avg	**687.5**
OUT	6	0.5	0.5	300	0.002	5.8	5.6	~~0.2~~	0.15	~~30.0~~
	7	0.5	1.5	300	0.005	5.9	5.5	~~0.4~~	0.15	~~50.0~~
	8	0.5	2.0	300	0.007	5.8	5.3	~~0.5~~	0.15	~~52.5~~
	9	0.5	3.0	300	0.010	5.8	5.1	~~0.7~~	0.15	~~55.0~~
	10	0.5	4.0	300	0.013	5.8	5.2	~~0.6~~	0.15	~~33.7~~
	11	0.5	5.0	300	0.017	5.9	4.1	~~1.8~~	0.15	~~99.0~~
	12	0.5	6.0	300	0.020	5.9	4.9	~~1.0~~	0.15	~~42.5~~
	13	0.5	8.0	300	0.027	5.9	4.6	~~1.3~~	0.15	~~43.1~~
	14	0.5	10.0	300	0.033	5.9	3.7	2.2	0.15	61.5
	15	0.5	12.0	300	0.040	5.9	3.4	2.5	0.15	58.8
									Avg	**60.1**

For MAP-SCMFC-A there was a 91.3% reduction in organic matter as shown in Table H-1.